Ecological Modelling 466 (2022) 109911

Contents lists available at ScienceDirect

Ecological Modelling

journal homepage: www.elsevier.com/locate/ecolmodel

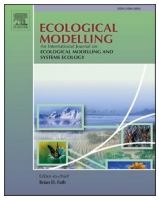

Incorporating temperature-dependent fish bioenergetics into a Narragansett Bay food web model

Margaret Heinichen [a,*], M. Conor McManus [b], Sean M. Lucey [c], Kerim Aydin [d], Austin Humphries [e,a], Anne Innes-Gold [e], Jeremy Collie [a]

[a] Graduate School of Oceanography, University of Rhode Island, 235 Coastal Institute Building, 215 South Ferry Rd, Narragansett, RI 02882, United States
[b] Rhode Island Department of Environmental Management, Division of Marine Fisheries, 3 Ft. Wetherill Rd., Jamestown, RI 02835, United States
[c] NOAA, National Marine Fisheries Service, Northeast Fisheries Science Center, 166 Water Street, Woods Hole, MA 02543, United States
[d] NOAA, National Marine Fisheries Service, Alaska Fisheries Science Center, 7600 Sand Point Way NE, Seattle, WA 98115, United States
[e] Department of Fisheries, Animal and Veterinary Sciences, University of Rhode Island, Kingston, RI, United States

ARTICLE INFO

Keywords:
Food web model
Fish bioenergetics
Rpath
Estuary
Climate change
Thermal responses

ABSTRACT

Food web models capture shifting species interactions, making them useful tools for exploring community responses to disturbances. The inclusion of environmental drivers, such as temperature, can improve model predictions, as energy demands of an organism can be temperature specific. While mass-balance models such as Ecopath with Ecosim (EwE) and the R implementation, Rpath, have included some thermal responses in past work, models have yet to include temperature-dependent energetic demands and metabolic costs. Our work demonstrates the inclusion of temperature-dependent bioenergetics into an Rpath food web model using the case study of a warming estuary: Narragansett Bay (Rhode Island, U.S.A). Thermal response parameters from literature were used to construct Kitchell curves describing temperature-dependent consumption and modified Arrhenius curves describing temperature-dependent respiration. Surface water temperature time series from 1994 to 2054 for high and low warming scenarios were created using observed temperatures and projections from the Coupled Model Intercomparison Project (CMIP6) multi-model ensemble. The integration of temperature-dependent fish bioenergetics resulted in lower projected biomasses as energetic demands increased. The degree to which biomass was impacted varied by functional group, though piscivorous fishes were particularly affected as both that group and their prey groups had forced bioenergetic changes. The differences in the model-predicted biomasses highlight the importance of accounting for thermal effects on marine species in ecosystem models, which will become increasingly important as ocean temperatures continue to rise in Narragansett Bay and elsewhere.

1. Introduction

Climate change represents a major continuous perturbation to the Northeast U.S. Continental Shelf ecosystem, affecting species distribution, migration phenology, and physiological processes (Chabot et al., 2016; Kleisner et al., 2017; Langan et al., 2021; Pershing et al., 2015). Increasing sea temperatures have been acutely observed in Narragansett Bay, Rhode Island (U.S.A), where surface water temperatures have risen approximately 1.5 °C since 1950 (Fulweiler et al., 2015). Climate-driven models can help elucidate how these changes in temperature are affecting ecosystem dynamics (Brander, 2015). Food web models created using implementations of the Ecopath and Ecosim algorithms (Polovina, 1984; Walters et al., 1997) are becoming increasingly popular to study how ecosystems respond to changes in fisheries harvest, species interactions, and other external stressors (Buchheister et al., 2017; Colléter et al., 2015; Villasante et al., 2016). While some Ecopath and Ecosim studies have included physical and environmental drivers (Bentley et al., 2017; Corrales et al., 2017; Hernvann et al., 2020; Serpetti et al., 2017), and other modeling platforms such as Atlantis (Audzijonyte et al., 2017) include broader interactions between the physical environment and species biology, direct impacts on species bioenergetic demands have not yet been incorporated into Ecosim-based food web models.

As ectotherms, fish rely on the environment to regulate their body

* Corresponding author.
E-mail address: mheinichen@uri.edu (M. Heinichen).

https://doi.org/10.1016/j.ecolmodel.2022.109911
Received 25 May 2021; Received in revised form 5 February 2022; Accepted 11 February 2022
Available online 19 February 2022

temperature, with ambient temperatures ultimately influencing physiological rates (Jobling, 1994). These individual-level metabolic processes and life history rates of organisms can scale up to impact ecosystems Humphries and McCann, 2014; Chabot et al., 2016). Consequently, bioenergetics and physiological responses are often used as the basis for mechanistically-driven models (Jørgensen et al., 2016). The basics of temperature-dependent bioenergetics have been recognized for decades (Brett, 1971; Jobling, 1994), and while species-specific rates are often unknown, it is nonetheless important to begin incorporating bioenergetic relationships into multispecies ecosystem models for increased realism of how species dynamics are affected by warming waters. Understanding community responses to climate change, rather than examining single-species responses in isolation, will provide more insight as to how environmental stressors will affect marine ecosystems (Nagelkerken and Munday, 2016).

As temperatures increase from the cooler portion of a species' thermal tolerance, it can become more energetically expensive for ectotherms to maintain base metabolic demands (Chabot et al., 2016; Jobling, 1994). The thermal response of metabolism is frequently described with an Arrhenius equation (Eq. (1)) if thermodynamic relationships are considered the dominant drivers (Brown et al., 2004; Gillooly et al., 2001; Schulte, 2015). The Arrhenius equation, often used in fitting laboratory data or in models incorporating metabolic ecology (Blanchard et al., 2012; Clarke and Johnston, 1999; Dahlke et al., 2020; Neubauer and Andersen, 2019), calculates the rate of reaction (k) as a function of a constant (A), the activation energy (E_a), the universal gas constant (R), and the temperature (T) in degrees kelvin.

$$k = Ae^{-E_a/RT} \tag{1}$$

Temperature-dependent energetic costs can modify species interactions, primarily through the adjustment of consumption rates as predators alter their intake to maintain their energy inputs (Johansen et al., 2015). In relation to temperature, consumption increases as waters warm, reaches a maximum at some optimum temperature, and then ingestion sharply decreases as the maximum tolerated temperature is approached (Fogarty and Collie, 2020; Jobling, 1994). Increasing consumption with increasing temperatures has been documented for a variety of fishes including bluefish (*Pomatomus saltatrix*), brook trout (*Salvelinus fontinalis*), and anemonefish (*Amphiprion melanopus*) (Buckel et al., 1995; Nowicki et al., 2012; Olla et al., 1985; Ries and Perry, 1995). Increased metabolic demand in warmer waters likely accounts for the increasing portion of the curve, while stress responses and behavioral shifts are thought to drive the reduced consumption rates frequently seen near species' thermal maxima (Brett, 1971; Jobling, 1997; Johansen et al., 2014; Nowicki et al., 2012). The exact shape can vary due to the many factors affecting consumption, such as locomotion, hormone regulators, detection, and successful prey capture, but numerous experimental studies have documented this general thermal response (Jobling, 1997; Volkoff and Rønnestad, 2020).

Higher energetic demands can adversely affect production, or the surplus energy available for optional processes such as growth and reproduction (Jobling, 1994; Neubauer and Andersen, 2019). Temperature can affect the efficiency with which organisms transform food energy into growth (Lemoine and Burkepile, 2012). Given that the foundational bioenergetic relationships apply to many marine species operating in their preferred thermal range (Deslauriers et al., 2017; Sibly et al., 2012), the integration of temperature-dependent bioenergetics in ecosystem models can provide more realistic predictions of how climate change will impact ecosystem production (McKenzie et al., 2016).

The Ecopath and Ecosim algorithms have been formated for use in multiple computer languages (Kearney, 2017). The popular Ecopath with Ecosim software (EwE; Christensen and Pauly, 1992; www.ecopath.org), a point-and-click implementation, has been used to model over 800 marine and aquatic ecosystems (Colléter et al., 2015; Lucey, 2019). The static, mass-balance Ecopath gives a snapshot of the energy flow of an ecosystem at a certain point in time. Ecopath uses master equations for consumption and production and requires data inputs of biomass (B), production-to-biomass ratio (P/B), consumption-to-biomass ratio (Q/B), a diet matrix, and fishing information (Christensen et al., 2005; Christensen and Pauly, 1992). Ecosim uses this food web snapshot as initial conditions to create time-dynamic projections of biomass (Coll et al., 2009). Predation is modeled with foraging arena theory in which prey are, at times, vulnerable to predation and invulnerable at others (Ahrens et al., 2012; Walters and Christensen, 2007). The vulnerabilities, or the parameters specifying the rate of exchange between vulnerable and invulnerable states, are estimated with a fitting procedure to minimize the sum of squares between projected and observed biomasses (Heymans et al., 2016). Ecosim-type models projected into the future can reach an equilibrium state if not forced by varying external inputs. External forcing functions of changing inputs, such as primary production or fishing effort, can also be used to drive the dynamic models into the future (Christensen and Walters, 2004).

The original Ecopath and Ecosim algorithms were not designed to include environmental forcing, such as temperature and nutrients. However, primary production can be forced based on environmental conditions (Guénette et al., 2006; Heymans et al., 2005), and recent enhancements have allowed researchers to incorporate a thermal modifier of species consumption (Bentley et al., 2017; Corrales et al., 2018; Guénette et al., 2014; Serpetti et al., 2017) or temperature-dependent recruitment (Bentley et al., 2020). The models with temperature-dependent consumption used temperature of occurrence data to estimate thermal preference, and modified consumption to restrict foraging capacity for each species or functional group. However, no implementation of Ecopath or Ecosim has so far incorporated the other major energetic impact of temperature: changing energy demands and metabolic costs. One of the master equations of Ecopath specifies that consumption in units of biomass consumed is the sum of production, respiration, and unassimilated food ($C = P + R + U$; Christensen et al., 2008). Metabolic costs are aggregated into the respiration term which represents the biomass lost to the ecosystem (i.e., energy that is consumed and assimilated by a group but is not transformed into production). The introduction of additional temperature-dependent bioenergetics in food web models creates an opportunity for further exploration of ecosystem response to shifting environmental conditions. In this paper, we explore changing energy demands and metabolic costs using a flexible implementation of Ecopath and Ecosim algorithms in the open-source R computer language, 'Rpath' (Lucey et al., 2020).

Rpath is the R implementation of the Ecopath and Ecosim algorithms. The data needs and modeling framework of Rpath are internally consistent with other iterations, such as the EwE software. The static Rpath uses a combination of inputs of biomass, consumption, production, and ectotrophic efficiency as well as a diet matrix, fishing information, and growth parameters for multi-stanza groups. The resulting mass-balance food web snapshot can be used to examine patterns of energy flow and interconnectedness of a food web. Rsim creates time dynamic biomass projections, modeling predation interactions using foraging arena theory described originally in Walters et al. (1997). Rsim projections can incorporate forced, or externally-driven, biomass, mortality, and fishing time series, among others. Output from Rsim allows for predictions of how populations may be directly or indirectly impacted by changing stressors and how those changes affect food web dynamics. The major advantage of the Rpath package is that all model code, including variations of the same model or different models, are held in the same script for ease of replication and analysis. The benefits and capabilities of the Rpath package are more fully described in Lucey et al. (2020).

The goal of this study is to investigate how temperature-dependent fish bioenergetics can influence food web dynamics, and how these physiological processes can be incorporated into ecosystem models

using Rpath. The inclusion of temperature-dependent bioenergetics may inform our inference on how the ecosystem will be altered with climate change. We apply this method to better understand top-down climate change impacts using the warming Narragansett Bay (Rhode Island, U.S.A) as a case study. We expand the functionality of Rpath and illustrate the scales at which temperature-dependent consumption and respiration can alter modeled biomass and food web structure.

2. Methods

2.1. Base model

Our work extended an existing EwE model of Narragansett Bay (Rhode Island, U.S.A; Fig. 1; Innes-Gold et al., 2020). Narragansett Bay is a productive, tidally-mixed estuary in the Southern New England area of the Northeast U.S. Shelf (McManus et al., 2020; Oviatt et al., 2017). There are both commercial and recreational fisheries as well as aquaculture, marine transportation, and general recreational uses (Dalton et al., 2010; Innes-Gold et al., 2021). Water temperatures have been rising in the last few decades, making Narragansett Bay an appropriate study site to investigate the impacts of climate change (Fulweiler et al., 2015).

The EwE model presented by Innes-Gold et al. (2020) provides a broad representation of Narragansett Bay suitable for a variety of questions, with an emphasize on upper trophic levels and fished groups. The model contains 15 functional groups (Supplemental Table A1.1), that include 28 species of commercial, recreational, or ecological importance assembled into the upper trophic level groups based on diet similarity. The starting conditions of the Ecosim model were averaged 1994–1998 data, including biomass from sampling programs within Narragansett Bay and scaled down state fisheries landings. The dynamic Ecosim model was fitted to annual-averaged observed biomass data from 1994 to 2018, so that each year was fitted to a single biomass value for that year. The model was forced with annual total commercial and recreational fishing mortality for the fished groups as well as the annual-averaged biomasses of phytoplankton and cultured shellfish, which were inputted as stepwise functions. The model used all annually-averaged inputs and did not include any seasonality components. The EwE model did not include any explicit environmental forcing. Further information on the model setup can be found in Innes-Gold et al. (2020).

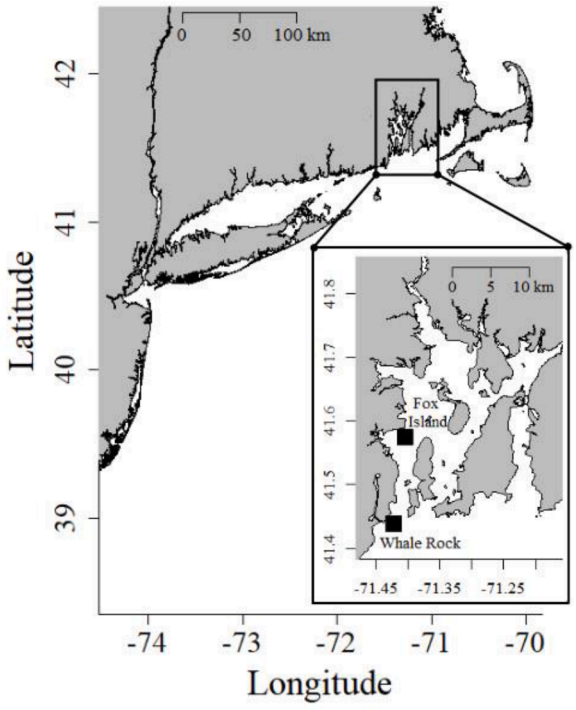

Fig. 1. Map of Narragansett Bay. The northern Fox Island station of the URI GSO fish trawl and the southern Whale Rock station are indicated as squares in the close-up map.

The Narragansett Bay EwE model was reformatted for compatibility with the R package 'Rpath' described in Lucey et al. (2020) using R version 3.6.0 (R Core Team, 2019). There were minor differences in the Rpath and EwE outputs because Rpath and EwE have slight differences in rounding and some default parameters, but there were no major changes to biomass trajectories, patterns, or relationships predicted because the modeling framework and underlying equations are internally consistent. The Rsim base model outputs the same main results of the EwE model described in Innes-Gold et al. (2020). The Narragansett Bay food web was highly connected, and nearly half of the energy of the system originated from detritus and deposit feeding benthos. In both the Rsim and Innes-Gold et al. (2020) Ecosim model outputs, the forced phytoplankton biomass was quite variable and particularly influential. While fishing mortality also varied throughout the time series, the large number of bottom-up vulnerabilities caused lower trophic functional groups to strongly follow the phytoplankton trends. The piscivorous and benthivorous groups had the best fits to observed data. In agreement with observed biomass data, nearly all groups increased in biomass between 1994 and 2018, though carnivorous benthos steadily declined in the same period. More specific information on the drivers of these patterns and the details of the functional group time series can be found in Innes-Gold et al. (2020).

Our Rsim model was projected from 1994 to 2054. The forcing functions of the original EwE model (i.e., phytoplankton biomass, cultured shellfish biomass, and fishing mortality; Supplemental Fig. A1.1) were held constant from 2019 to 2054 at the present-day levels (average of the 2014–2018 values; Supplemental Table A1.3) to isolate the impacts of shifting bioenergetics on the food web. Further details on the Rpath and Rsim inputs can be found in Supplement A.1. The Rsim output projected through 2054 without temperature forcing was considered the 'base' version of our model.

For the model versions with temperature-dependent bioenergetics, thermal responses were only included for the finfish functional groups (planktivorous fish, benthivorous fish, and piscivorous fish). There is currently greater availability of bioenergetic data for the modeled fish species compared to the invertebrate species, and the thermal responses of other taxa may be best represented with different functional forms than those used for fish. Thermal response parameters were obtained from literature for each of the 19 species that compose the fish functional groups (Supplemental Table A1.2).

2.2. Temperature

Surface water temperatures were taken from the University of Rhode Island Graduate School of Oceanography (URI GSO) weekly fish trawl (Collie et al., 2008). Before 2007, temperature was measured with a thermometer from water samples collected at the surface and bottom; since 2007 a YSI® (Model 6920 V2) multi-parameter water quality sonde has been used (University of Rhode Island Graduate School of Oceanography, 2021). Occasional missing temperatures were estimated based on imputations calculated from generalized additive models (GAMs) as described in Langan et al. (2021). Only the temperatures recorded from the Fox Island station (~7 m depth) were used in our study, as this mid-bay station was thought to better represent average of the temperatures experienced in Narragansett Bay than the lower bay Whale Rock station (~20 m depth; Fig. 1). Surface temperature was examined instead of bottom temperature because both benthic and pelagic fish species were assessed, and fewer correlations were needed to predict surface water temperature in the projections through 2054. Since the food web model was based on annual-averaged data (i.e. either using a single value for a year or a stepwise function where all months of the year used the same

yearly-averaged value), annual average temperatures from 1994 to 2018 were calculated as the average of each monthly temperature to account for unequal sampling effort in some months.

Temperature projections for Narragansett Bay were constructed to discern how the Narragansett Bay ecosystem may change in the future when accounting for temperature-dependent bioenergetics. First, grid cells' data which included Narragansett Bay from six models of the Coupled Model Intercomparison Project 6th phase (CMIP6) multi-model ensemble were accessed. The two warming scenarios tested were a low warming scenario from Shared Socioeconomic Pathway 1-2.6 (SSP1-2.6) and a 'business as usual' high warming scenario with SSP5-8.5 (O'Neill et al., 2016; Eyring et al., 2016; Supplemental Table A2.1). The air temperature projections from the six CMIP6 models were delta corrected and linearly transformed to project yearly averaged surface water temperatures following the methods described in Bell et al. (2018). To bias correct the projections, delta corrections were applied between the CMIP6 modeled air temperature and observed air temperature as well as observed water temperature and projected water temperature. Air temperature data from the National Oceanic and Atmospheric Administration (NOAA) National Centers for Environmental Information for the TF Green Airport, Providence, RI station were used to relate observed air temperature to observed surface water temperatures (www.ncdc.noaa.gov; Supplemental Table A2.2). Temperatures were projected through 2054 based on data availability. This projection timeframe is long enough to see distinct changes in the average temperature, while being short enough to provide reasonable projection results, since physiological responses can adjust on shorter timescales through acclimation (i.e., physiological adjustment to new, sustained conditions) and adaptation, and on longer timescales (i.e., yearly to decadal) through range shift, ecological feedbacks, and evolution (Peck, 2011; Sibly et al., 2012). The final time series for the high and low warming scenarios were created by averaging the six delta-corrected surface temperature projections for each year after 2018. These temperature time series were used with thermal response curves to create time series of modifier values to functional group consumption and respiration described in the following sections.

2.3. Temperature-dependent consumption

The food consumption thermal response for each of the three fish functional groups was described using the Kitchell equation (Hansen et al., 1997; Kitchell et al., 1977), which is routinely used to characterize temperature-dependent consumption in bioenergetic models (Hansson et al., 1996; Harvey, 2009; Luo and Brandt, 1993). The Kitchell equation, shown in Eq. (2), uses straightforward input parameters of the thermal maximum (T_{max}; the temperature above which consumption is zero), temperature of optimum consumption (T_{optC}), and the Q_{10} of consumption (referring to the rate of change for a process as the temperature increases 10 °C; Hansen et al., 1997; Fogarty and Collie, 2020) to estimate the proportion of maximum consumption that occurs at a given temperature (r_c).

$$r_c = \left[\frac{T_{max} - T}{T_{max} - T_{optC}}\right]^X * e^{\left[X*\left(1-\frac{T_{max}-T}{T_{max}-T_{optC}}\right)\right]} \quad (2)$$

$$where\ X = \left\{\frac{\left[\ln(Q_{10})*\left(T_{max} - T_{optC}\right)\right]^2}{400}\right\} * \left\{1 + \left[1 + \left(\frac{40}{\ln(Q_{10})*\left(T_{max} - T_{optC} + 2\right)}\right)^{0.5}\right]^2\right\}$$

The three thermal parameters (T_{max}, T_{optC}, Q_{10}) for each fish species were derived from the literature, and a hierarchy of data sources was used to choose the value for each parameter (Supplement A.3). The original Innes-Gold et al. (2020) model was parameterized for adult fish; for compatibility, literature values for adults were chosen over those for younger life stages. Additionally, experimental studies were chosen over values reported from other models. For each species, T_{max} was chosen as the highest value from temperature of occurrence data in Narragansett Bay, stock-wide temperature of occurrence from the website Aquamaps (Kaschner et al., 2019; www.aquamaps.org), or studies focusing on thermal tolerance. For some species, limited information required the assumption of relationships between T_{optC}, T_{max}, and a described temperature of maximum growth to estimate T_{optC} in the absence of published consumption data. The Q_{10} was assumed to be 2.3 when no other estimate was available (Hansen et al., 1997). Effort was made to choose values from studies that were the most representative of the fish in Narragansett Bay, but, particularly in the case of T_{optC}, we were limited by the information available in the literature.

Consumption thermal response by functional group began with the species-specific Kitchell input parameters. A biomass-weighted average of species from 1994 to 1998 (Supplemental Table A3.4) yielded the parameters by functional group, which were then inputted to the Kitchell equation. The weighting of the consumption curve, therefore, was weighted the same as the other original Ecopath parameters (Innes Gold et al., 2020). Modeling bioenergetic responses on a functional group level smoothed intra- and inter-species variability in thermal response. The challenge of determining an appropriate level of aggregation when integrating physiological responses in models has been recognized by others (Cooke et al., 2014), but our method was the most consistent with the parameterization of the original EwE model.

We ran a sensitivity test to examine the effect of input community composition on the consumption thermal response curves (referred to as the community composition sensitivity test). Three Kitchell curves per functional group, weighted by different species biomasses, were used to create consumption modifier time series; (1) the 1994–1998 averaged biomasses as described earlier in the methods, (2) the single year's observed biomass from the time series data that resulted in the strongest warm-skewed curve, and (3) biomasses including more southern, warm-water species to represent a future curve as new species enter Narragansett Bay. Further information on the creation of the curves with southern species can be found in Supplement Table A4.1. The three Kitchell curves were inputted into the high warming consumption version of the model to compare resulting fish biomasses.

The thermal response curves were adjusted to account for the temperature at which the Innes-Gold et al. (2020) Ecopath equilibrium baseline was established. The standard Kitchell curve ranges between zero and one. In this food web modeling framework, the time dynamic model uses the static Rpath model as the starting conditions. In our case, the Rpath model represented the average ecosystem state in 1994–1998, and the input parameters capture average values rather than extremes. The standard Kitchell equation would use our Q/B value as a maximum consumption, which would be incorrect and not allow the option for consumption to increase over time. Since the Q/B input values represent an actual consumption rather than a maximum, it was necessary for us to scale the Kitchell curve so that it could increase above one and allow consumption to increase. The scaling of the curve grounded the thermal response in the starting conditions of the initial Rpath model, the average 1994–1998 temperature of the Bay (T_{B94}). We scaled the

Kitchell curve by dividing by the Kitchell curve value at the average 1994–1998 Bay temperature ($r_c|_{TB94}$), so that the thermal modifier was 1.0 at T_{B94} (Eq. (3)). The scaled Kitchell curve, referred to as the relative consumption curve (r_c_scaled), had a maximum consumption modifier greater than one at T_{optC}. The time series of annual consumption modifiers were then calculated by evaluating the relative consumption curve at the average temperature from each year of the time series.

$$r_c\_scaled = r_c \Big/ \left(r_c|_{T_{B94}}\right) \tag{3}$$

The base model with temperature-dependent consumption will be referred to as the 'consumption' version of the model. In this study, the consumption modifiers were applied with the 'ForcedSearch' feature of Rpath (formerly called 'ForcedPred'). This forcing option modifies the effective predator biomass which is then inputted into the main consumption calculations (Lucey et al., 2020). The ForcedSearch function calculations apply the thermal response before the full consumption calculations, so that the foraging arena and interspecies interactions mediate the temperature effect on physiological processes, as has been suggested previously (Neubauer and Andersen, 2019). To remain consistent with the parameterization and forcing of the original EwE model, the consumption version of the model was forced with a stepwise time series of the consumption modifier, in which each year was forced with the modifier as calculated for that year.

2.4. Temperature-dependent respiration

The second bioenergetic response built into Rpath was temperature-dependent respiration. Respiration was treated similarly to standard metabolism, though respiration includes other energetic costs such as specific dynamic action (SDA), the metabolic cost to digest food, and activity costs. Our framing of metabolism as the amount of energy used to maintain function was more directly applicable to the mass-balance setup and respiration term than other metrics such as aerobic scope. The original Innes-Gold et al. (2020) EwE model was a parsimonious model of the ecosystem in which species age and size were generally not included. Therefore, our functional form for temperature-dependent respiration was simplified because it did not include a body mass effect on respiration (Sibly et al., 2012). This simplification was appropriate since the fish groups in the base model were not multi-stanza (i.e., subdivided into size or age groups), and size structure of the population was not modeled.

Though the literature often describes respiration as an exponential increase of base metabolic energy demand with temperature, many experimental studies only reported two- to four-fold increases in standard or resting metabolism (Bernreuther et al., 2013; Dalla Via et al., 1998; Johansen and Jones, 2011; Sandersfeld et al., 2017; Schwieterman et al., 2019; Slesinger et al., 2019; Stewart and Binkowski, 1986). Studies investigating the relationship between temperature and metabolic costs have included SDA or locomotion, but similar ranges of metabolic increases were reported (Fu et al., 2009; Hartman and Brandt, 1995). Therefore, we thought that including resting metabolism, SDA, and activity should only increase energetic losses to metabolism by a factor of eight to ten-fold over biologically relevant temperatures.

The modified Arrhenius equation reported in Blanchard et al. (2012) calculated with their reported parameters was used as the functional form for the thermal response of fish respiration in relationship to temperature (Eq. (4)). The thermal modifier (τ), ranging from zero to ten, is a function of the temperature in degrees kelvin, the Boltzmann constant (k; 8.62×10^{-5} eV K^{-1}), the activation energy (0.63 eV; similar to values in other studies such as Gillooly et al., 2001; Brown et al., 2004), and a constant ($c1$=25.55).

$$\tau = e^{c1-(E/kT)} \tag{4}$$

The modified Arrhenius equation is the best fit for constraining the metabolic modifier to the range of increases seen in literature for these and similar species. However, there are no species-specific parameters. Given that any species-specific thermal responses would be clouded in the base model's aggregation to functional groups, we considered the Blanchard et al. (2012) equation to adequately represent a generalized (i.e., non-species specific) fish metabolic thermal response. The respiration thermal response was scaled using similar methods to the consumption response scaling, so that a modifier of τ=1 on the relative respiration curve (τ_{scaled}; i.e., scaled Blanchard curve) was associated with T_{B94} (Eq. (5)).

$$\tau_{scaled} = \tau \Big/ \left(\tau|_{T_{B94}}\right) \tag{5}$$

In the default programming of Ecopath and Rpath, production rate (P/B) is a specified static value, and respiration is solved for. Rsim uses a parameter, *ActiveRespFrac*, to represent the fraction of energy devoted to respiration. It is calculated as a proportion of energy remaining after production (estimated using the production-to-consumption ratio of the Rpath output; P/Q) and unassimilated food is accounted for (Aydin et al., 2016). The *ActiveRespFrac* parameter is used throughout the dynamic Rsim simulations. Unassimilated food is assumed to be independent of temperature.

The first step in creating the time series used to force temperature-dependent respiration was to multiply the relative consumption curves by the Rpath total consumption, equal to Rpath Q/B multiplied by biomass, to make a curve of total consumption by temperature (*TotCons*; Eq. (6)).

$$TotalCons = r_c\_scaled * Q/B_{Rpath} * Biomass_{Rpath} \tag{6}$$

The total consumption at T_{B94} for each of the functional groups was multiplied by the *ActiveRespFrac* of the base Rpath model to get the total respiration at T_{B94} ($TotResp_{T_{B94}}$; Eq. (7))

$$TotalResp_{T_{B94}} = TotalCons|_{T_{B94}} * ActiveRespFrac_{Base} \tag{7}$$

The relative respiration curve was multiplied by the ratio of the total respiration at T_{B94} to the relative respiration modifier value at that temperature which produced a total respiration by temperature curve (*TotalResp*; Eq. (8)).

$$TotalResp = \tau_{scaled} * TotalResp_{T_{B94}} \Big/ \tau_{scaled}|_{T_{B94}} \tag{8}$$

Dividing the total respiration by total consumption gave *ActiveRespFrac* by temperature (Eq. (9)). Using this curve and the temperature time series, we calculated the ActiveRespFrac for each year in the time series.

$$ActiveRespFrac = TotalResp/TotalCons \tag{9}$$

We scaled the consumption and respiration curves to the temperatures that informed the original parameters estimated in the Rpath model to examine the sensitivity of the curves to the implicit thermal parameterization of the Rpath model and different scaling temperatures. In this sensitivity test (referred to as the scaling temperature sensitivity test), the Kitchell curves were scaled to the temperature informing the Q/B parameters (T_{QB}; see Supplement A4 for more information) instead of the temperature of the Bay (T_{B94}). The Blanchard curve was scaled by the temperature of fishing mortality (T_F; $T_F = T_{B94}$ as the fisheries catches used to calculate fishing mortality were taken from the Bay) and the temperature of natural mortality (T_M), as the P/B parameter is estimated as total mortality (T_Z = mean(T_F, T_M) = T_{PB}). The average temperatures informing the parameters for the fish functional groups can be found in Supplemental Table A4.2. Both the consumption and respiration versions of the model under the high warming scenario were compared under the scaling temperature sensitivity test.

To implement this temperature dependency, a new forcing function was developed, *ForcedActResp*, and added to the Rpath model (github.com/NOAA-EDAB/Rpath). The annual respiration modifier at each year, inputted through *ForcedActResp*, was calculated so that

ActiveRespFrac for each year matched what was predicted by the temperature time series and the *ActiveRespFrac* by temperature curves (Eq. (10)).

$$ForcedActResp = ActiveRespFrac \;/\; ActiveRespFrac_{Base} \quad (10)$$

This forcing function modifies the total energetic losses to respiration (*ActiveRespLoss*; Eq. (11)). The loss to respiration is a function of the energy gained from consumption and the fraction of energy devoted to respiratory costs.

$$ActiveRespLoss = FoodGain * ActiveRespFrac * ForcedActResp \quad (11)$$

2.5. Comparison of model versions

Three model versions with two warming scenarios for the temperature-dependent versions were compared (Table 1). The static starting condition of all model versions was the Rpath translation of the 1994–1998 average Ecopath model by Innes-Gold et al. (2020). The Rsim translation of the Innes-Gold et al. (2020) Ecosim model of Narragansett Bay is considered the 'base' version of our model. Temperature-dependent consumption only was included in the consumption version of the model, and both temperature-dependent consumption and respiration were included in the respiration version of the model (Fig. 2). The consumption and respiration versions were forced with observed annually-averaged temperatures from 1994 to 2018. Two warming scenarios, high and low, of annually-averaged temperatures were used to project the consumption and respiration model versions from 2019 to 2054. Versions of the model were compared in terms of fit (i.e., sum of squares between Rpath modeled absolute biomass and observed biomass), realism of bioenergetic responses to temperature, and future projected biomasses. The emphasis of our analysis surrounded the differences between model versions, focusing on 2019–2054 projections from the high and low temperature scenarios. Highlighting the differences between model version projections demonstrates how different methods of incorporating temperature-dependent bioenergetics can yield varying model outputs.

Table 1
Naming convention and descriptions of the base and temperature-dependent versions of the Rpath implementation of the Narragansett Bay food web model.

Model Version	Description	Temperature Scenarios Run	Sensitivity tests run
Base	Rsim translation of Innes-Gold et al. (2020) Ecosim model. Model version used the same fishing and biomass forcing as the Ecosim model.	No temperature forcing from 2019 to 2054.	None
Consumption (Cons)	Built on the base version of model run with temperature-dependent consumption only. Consumption modifiers applied using the *ForcedSearch* forcing function. Observed temperatures used for the 1994–2018 projections.	Two runs from 2019 to 2054: High warming & Low Warming	Community composition & scaling temperature (high warming scenario only)
Respiration (Resp)	Built on the consumption version of the model run with temperature-dependent respiration. Respiration modifiers applied using the new *ForcedActResp* forcing function. Observed temperatures used for the 1994–2018 projections.	Two runs from 2019 to 2054: High warming & Low Warming	Scaling temperature & vulnerability (high warming scenario only)

The third and final sensitivity test performed examined the influence of the vulnerability parameter (referred to as the vulnerability sensitivity test), given that we expected the vulnerability parameters to have strong impacts on resulting biomasses. Ecosim vulnerability parameters control the rate of exchange between vulnerable and invulnerable states in the foraging equations used to estimate predator *Q/B* (Walter et al., 1997; Aydin, 2004). The vulnerability values used in the base model are listed in Supplemental Table A4.3. The Qlink values (i.e., consumption from a predator to a specific prey) for which the fish were predators and output biomasses in the respiration model version with the high warming scenario were compared for three sets of vulnerabilities: the original values used in the Innes-Gold et al. (2020) model, a 20% change in vulnerabilities whereby each vulnerability was adjusted 20% closer to the default of 2, and the default 2.0 for all vulnerabilities.

3. Results

3.1. Temperature

There was strong interannual variability in the observed, annually-averaged surface temperatures from 1994 to 2018 (Fig. 3). The average 1994–1998 temperature of the Bay, T_{B94}, temperature was 11.7 °C. The historical temperatures of the CMIP6 models were generally comparable to observed temperatures. Each CMIP6 model had similar variability to the observed time series which was dampened when averaging the climate models together. However, this forward projection with lower variability still captured warming trends presented by the multi-model ensemble. The high warming scenario, SSP5-8.5, provided an overall increase of nearly 3 °C between the start of the time series and 2050. The low warming SSP1-2.6 initially projected higher temperatures than the SSP5-8.5, though overall only yielded an average increase of approximately 2 °C by 2050. The greatest difference between the high and low warming scenario projections was 1.1 °C in 2045.

3.2. Consumption response curves

The thermal response curves for consumption generally reflected the convex dome shape as suggested by theory (Fig. 4A). The curves varied between functional groups with piscivorous fish having the steepest increase in consumption below T_{optC}, while benthivorous fish had the steepest decrease near their thermal maximum. The input species for these curves generally had broad thermal tolerances, and the average temperatures experienced in Narragansett Bay were on the lower end of their tolerance ranges (Supplemental Fig. B2.1).

The thermal modifiers of all functional groups increased over the1.0 baseline early in the time series, though within each functional group the modifier only varied by 0.2–0.5 (Fig. 4B). The ending consumption modifier was larger in the high warming scenario for all fish groups, and piscivorous fish had the largest consumption modifier overall (maximum=1.38). The community composition sensitivity test resulted in relative consumption curves with different thermal maxima, but the consumption modifier time series were similar as the curves overlap at the colder average temperatures of the Bay (Supplemental Fig. B2.2). The most warm-skewed curves created from a single year's observed biomasses of the current fish species were more extreme than the curves created with moderate biomasses of new southern species that may enter the Bay in the future.

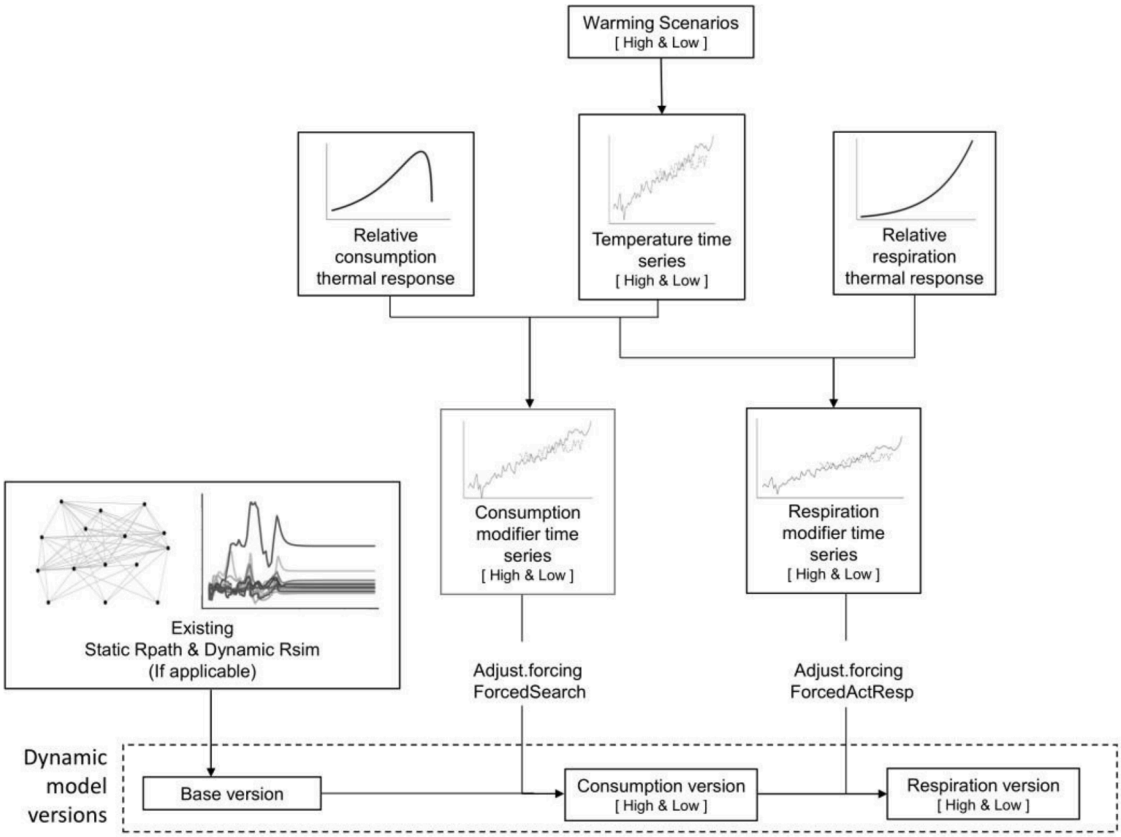

Fig. 2. Conceptual diagram for the inclusion of temperature-dependent bioenergetics into an Rpath with Rsim model. This work introduces the ability to adjust active respiration by applying a *ForcedActResp* forcing function.

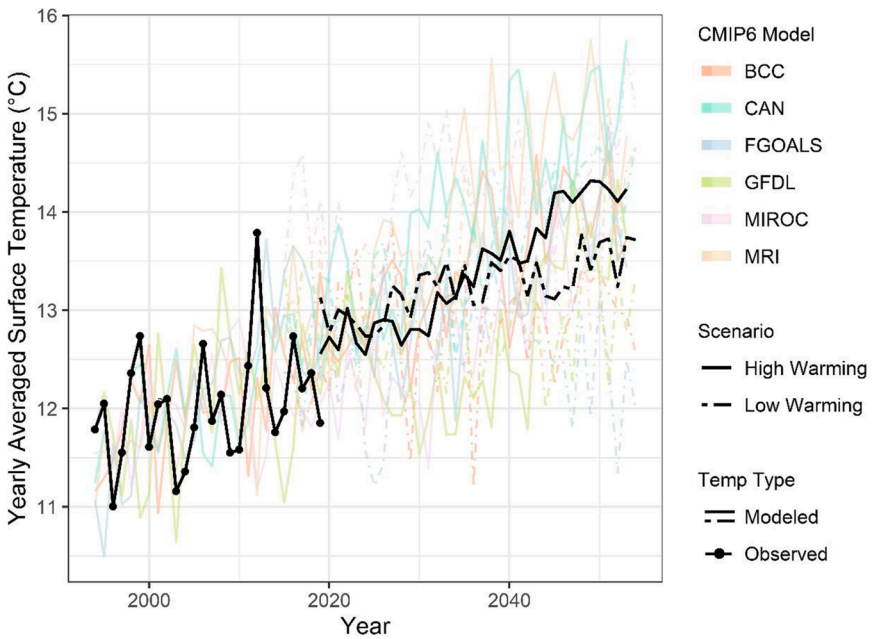

Fig. 3. Temperature time series inputs for the temperature-dependent model versions. The black line with points between 1994 and 2018 is the observed yearly average surface temperature of the GSO Fox Island fish trawl station. The colored lines are the six CMIP6 models (Supplemental Table A2.1). Solid lines are the high warming scenario and the dashed are the low warming scenarios. The projected Narragansett Bay surface temperatures for high warming (solid black line) and low warming (dashed black line) are the means of the six CMIP6 models. A table showing the values of the final temperature time series can be found in Supplemental Table B1.1.

3.3. Respiration response curves

The original Blanchard curve had a thermal modifier of 1.0 at 13 °C, thus the Blanchard curve and the relative respiration curve scaled to T_{B94} were similar (Fig. 5A). The three *ActiveRespFrac* curves by temperature varied by functional group due to the interplay between the respiration and consumption curves (Fig. 5B). The planktivorous fish *ActiveRespFrac* curve was relatively flat before steeply increasing near maximum temperatures. The benthivorous fish curve showed an increasing trend as waters warm (from 0.54 at 0 °C to 0.74 at 20 °C). The piscivorous fish *ActiveRespFrac* decreased to a minimum of energy allocated to metabolism (41%) occurring at 18.4 °C before sharply

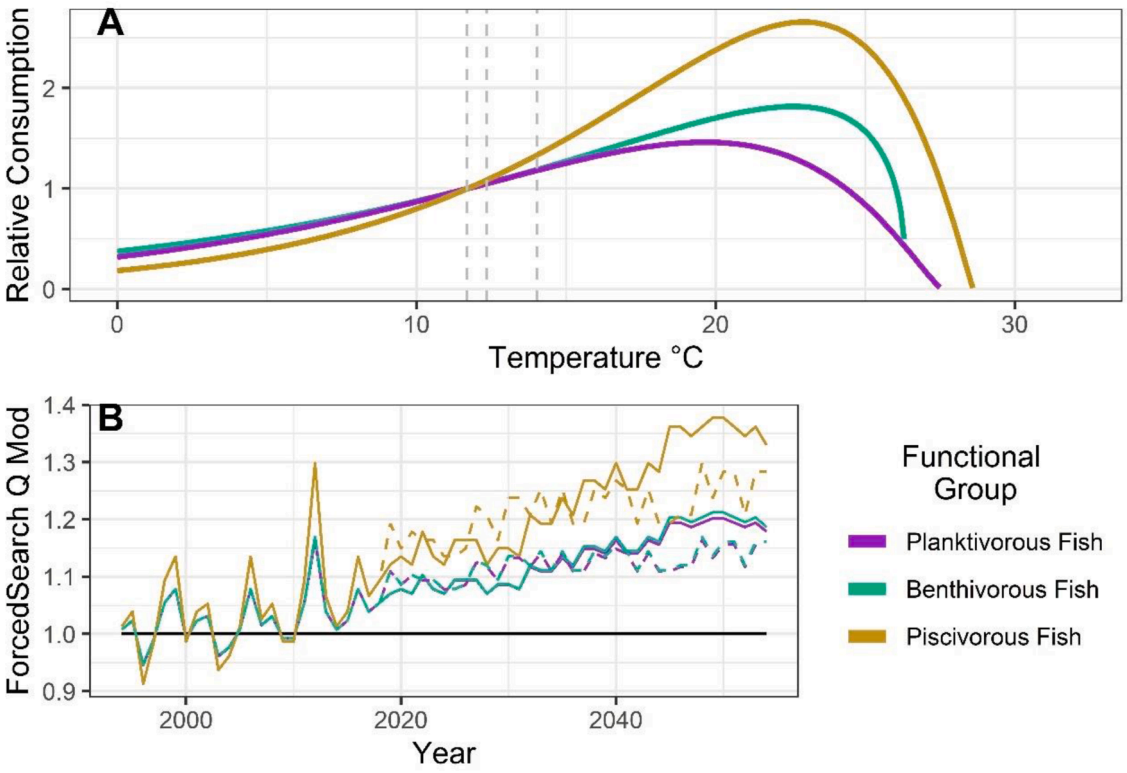

Fig. 4. Consumption thermal responses and modifiers. A) The relative consumption curves by functional group in response to temperature. Vertical gray dashed lines have been added to show T_{B94} (11.7 °C), the 2018 observed average temperature (12.4 °C), and the 2054 average temperature as projected under the high warming scenario (14.0 °C). B) The consumption modifier time series applied via the ForcedSearch function in the temperature-dependent versions of the model. Beyond 2018, the solid line is the modifier in response to the high warming scenario and the dashed lines reflect the low warming scenario. The default ForcedSearch of the base model is 1.0, shown by a black line.

increasing. The temperature-dependent production, shown by the balance of temperature-dependent consumption and respiration, varied in shape by functional group (Supplemental Fig. B3.1A– C). Piscivorous fish had the most defined temperature-production curve, in which the temperature of maximum potential production was slightly cooler than the temperature of maximum consumption. The planktivorous fish production-temperature curve was less pronounced, and there was a very minor curve in the energy available for production for benthivorous fish.

ActiveRespFrac forcing varied between the high and low projected warming scenarios (Fig. 5C). In the base version of the model, piscivorous fish had the lowest *ActiveRespFrac* (0.48), followed by planktivorous fish (0.53), and benthivorous fish had the highest (0.61). Both planktivorous fish and benthivorous fish *ActiveRespFrac* only varied by 0.03 throughout the time series. Both groups had higher ending metabolic demands compared to the starting conditions of the Rpath model. Unlike the other two functional groups, piscivorous fish *ActiveRespFrac* declined during the 60-year projection, as the temperatures experienced by the Bay during this period were still on the decreasing portion of their *ActiveRespFrac* curve.

Under the scaling temperature sensitivity test, the functional groups had different temperatures to scale the relative consumption and respiration curves. The T_{QB} for piscivorous fish was much higher than T_{B94} (Supplemental Table A4.2), which was reflected in the relative consumption curve for that functional group (Supplemental Fig. B3.2A). The consumption for piscivorous and benthivorous fish remained below the respective Rpath starting points for the entirety of the time series (Supplemental Fig. B3.2B). For respiration, the T_{PB} was similar to T_{B94}, so that the *ActiveRespFrac* by temperature curves differed slightly (Supplemental Fig. B3.3A,B). The *ActiveRespFrac* time series had similar increasing or decreasing patterns by functional group but were scaled differently relative to the initial *ActiveRespFrac* (Supplemental Fig. B3.3C). In this test, piscivorous fish had respiration costs higher than their baseline in all years.

3.4. Comparison of model versions

The inclusion of temperature-dependent fish bioenergetics impacted the modeled biomasses (Fig. 6, Supplemental Fig. B4.1). For planktivorous and benthivorous fish, the consumption model versions yielded higher ending biomasses than the base model, and the respiration model versions yielded lower biomasses in warming water (Fig. 7). Planktivorous fish and benthivorous fish biomasses were 14.55 g/m^2 and 9.93 g/m^2 in the high warming respiration version compared to 17.03 g/m^2 and 12.46 g/m^2 in the high warming consumption version. Piscivorous fish biomass was highest in the high warming respiration model version (9.25 g/m^2) due to their respiration costs decreasing as water temperature increased from its current state. As with the base model, the overall biomass trends for all groups are strongly driven by the forced phytoplankton biomass and fishing mortality. However, in the consumption and respiration model versions, the influence of the thermal drivers is evident.

Piscivorous fish had the greatest percent difference in the 2054 biomass estimates between the five tested model versions and scenarios (28% between the highest biomass in the high warming respiration version and the lowest biomass in the base version of the model). The other fish groups varied by 14.6% (planktivorous fish; highest biomass in high warming consumption version and lowest biomass in high warming respiration version) and 20.3% (benthivorous fish; highest biomass in high warming consumption version and lowest biomass in high warming respiration version). The carnivorous benthos group differed by 20.4% at most, with biomasses approximately 2 g/m^2 lower

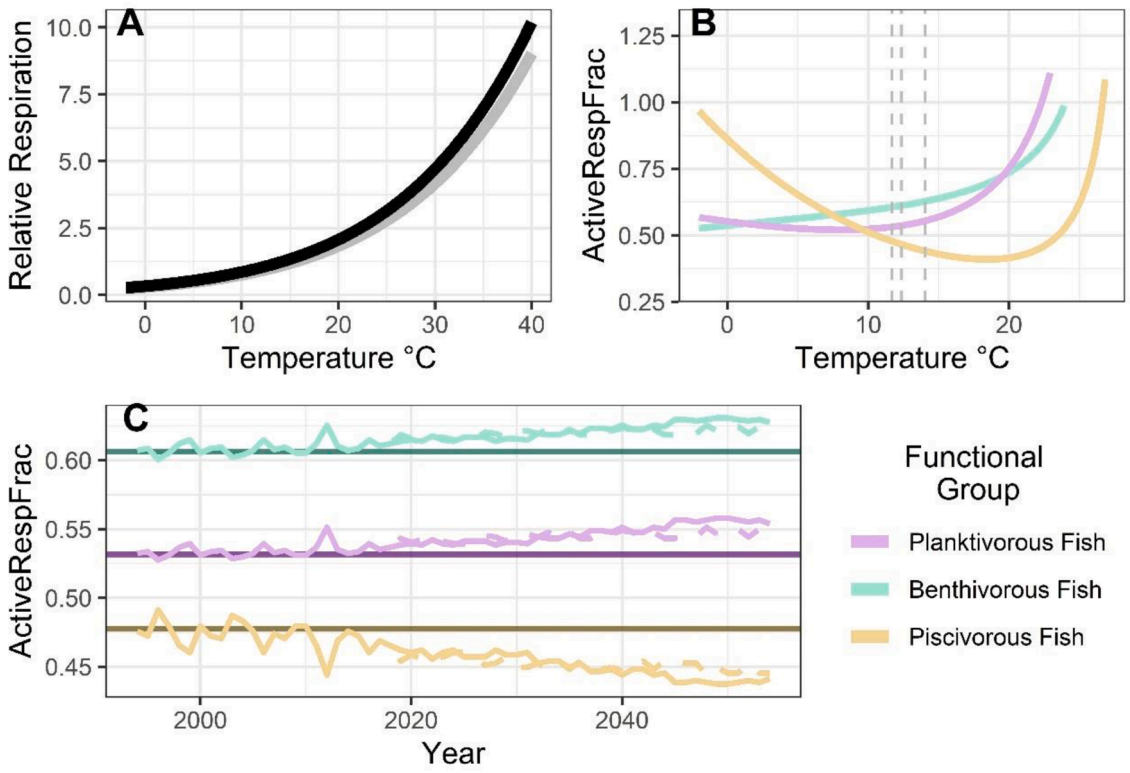

Fig. 5. Respiration thermal responses and modifiers. (A) The relative respiration curve used for all fish functional groups (black) compared to the original Blanchard curve (gray). (B) *ActiveRespFrac* (i.e., Rpath parameter value representing fraction of energy devoted to respiratory costs) by temperature for each functional group, as calculated from total respiration divided by total consumption. Vertical gray dashed lines have been added to show T_{B94} (11.7 °C), the 2018 observed average temperature (12.4 °C), and the 2054 average temperature as projected under the high warming scenario (14.0 °C). (C) *ActiveRespFrac* as a time series. The horizontal dark lines show the static *ActiveRespFrac* of the base version of the model. The solid pale lines after 2018 show the *ActiveRespFrac* in the high warming scenario and the dashed lines are for the low warming scenario.

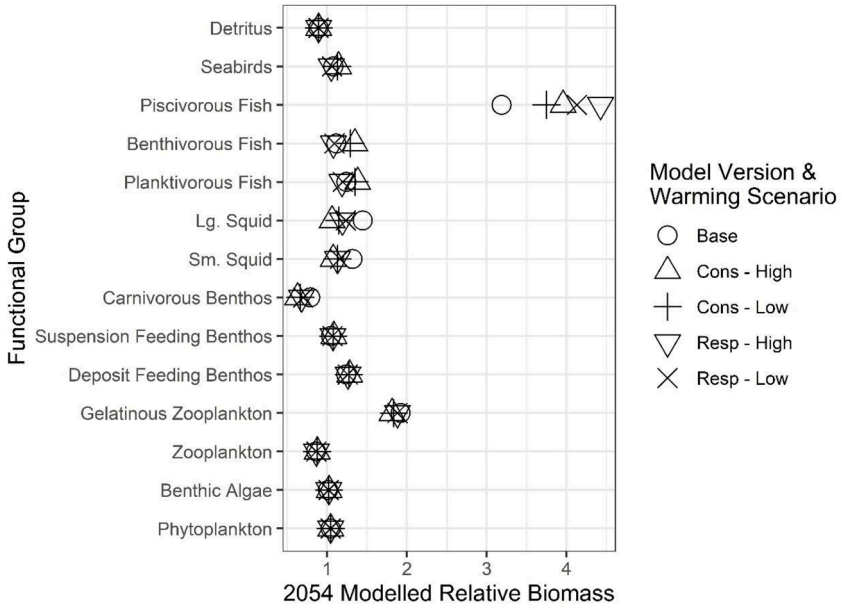

Fig. 6. Ending 2054 biomass outputs projected by Rsim relative to starting biomasses as defined in Rpath for the three model versions and two warming scenarios. The cultured shellfish group is not included. The biomass for that group was forced and increased by orders of magnitude, not aligning with the other groups plotted.

in the high warming consumption version than the base version (Fig. 6). Although their absolute biomasses were small, squid groups differed by 18–27% between model versions, with the base model version predicting the highest biomasses. These groups had stronger connections to the adjusted fish groups than the other mid and lower trophic level groups which had biomass vary between model versions by 1–6%.

The model version with the best fit (i.e., lowest sum of squares) varied by functional group (Supplemental Table B4.1). The consumption

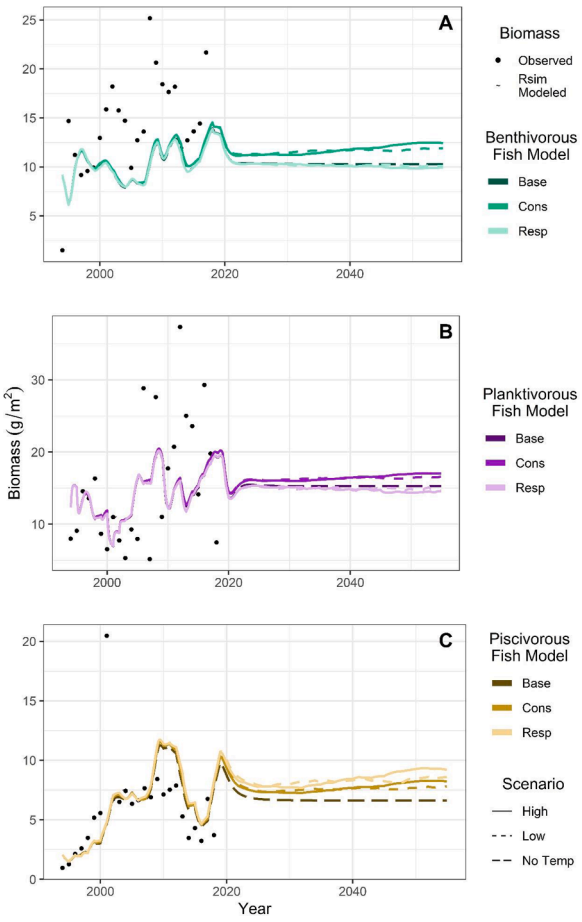

Fig. 7. Projected fish biomasses. Biomass trajectories (lines) for the three fish functional groups of benthivorous fish (A), planktivorous fish (B), and piscivorous fish (C) compared to the observed time series (points) used by Innes-Gold et al. (2020) to fit the original Ecosim model. Colors represent the model version and line type indicates the warming scenario. The base model run without temperature forcing is indicated with the no temperature scenario option.

version of the model gave the best fits for benthivorous fish, planktivorous fish, and carnivorous benthos, while the base version without environmental forcing had the lowest sum of squares for piscivorous fish and the squid groups.

In the community composition sensitivity test, the introduction of new species shifted the thermal maxima for the functional group, but, because of the cooler average temperature compared to the maxima, we did not see the difference in the relative consumption curves reflected in the biomass projections (Supplemental Fig. B4.2). There was limited variation in the 2054 biomasses projected under the scaling temperature sensitivity test (Supplemental Fig. B4.3). The base version of the model generally had higher biomasses than those forced with temperature-dependent bioenergetics scaled to T_{QB} and T_{PB}.

In the model versions, many of the vulnerabilities of strong predation connections for the fish groups were less than 2.0, which corresponds to bottom-up forcing. In the vulnerability sensitivity test, we made these important vulnerabilities more top-down (i.e., closer to 2.0), such that the fish groups were able to further increase their consumption (Supplemental Figs. B4.6.4–B4.6). Planktivorous fish, in particular, had higher projected biomasses when vulnerabilities were more top-down (Supplemental Fig. B4.7). The smaller changes in vulnerabilities between the fitted and 20% change in vulnerabilities yielded smaller changes in biomass (Supplemental Fig. B4.8).

All model versions had an ending *ActiveRespLoss* (energetic losses due to respiration; see Eq. (11)) higher than that of the static Rpath model (Table 2). There were noticeable, but not strong, differences in the 2054 respiration losses, reflecting the variability of the ending respiration modifier and biomasses between model versions.

As the forced temperatures only had minor variability and other main inputs of phytoplankton and fishing mortality were held constant, the total energy inputs and outputs had nearly equilibrated by 2054 in all model versions, and there were only slight variations in community metrics between model versions (Supplemental Table B4.2). Given that fish groups represent just a portion of the biomass of the ecosystem, certain ecosystem metrics, such as catch, were more strongly influenced by changing fish bioenergetics than others. The respiration model versions had the highest total ecosystem respiration and the lowest overall production.

4. Discussion

We have expanded an existing food web modeling platform to make a bioenergetics-based, temperature-dependent, food web model and have shown that this new functionality introduced into the flexible Rpath R package can affect biomass projections. Climate change elicits complex responses from organisms and ecosystems (Roessig et al., 2004), and our work adds a critical modeling component of temperature-dependent energetic losses. The inclusion of these physiological responses grounded in bioenergetic theory was shown to influence projected biomass output in the Rsim model. Our methodology can be used in combination with other tools to better predict the impacts of warming water on marine food webs.

4.1. Temperature

The effects of rising temperatures are increasingly being incorporated into fisheries and ecosystem models (Barange et al., 2018). Our temperature time series indicated that Narragansett Bay is likely to warm over the next few decades, similar in scale to what has been projected for other Atlantic U.S. estuaries (Muhling et al., 2018). Our methodology in Rpath can be used to force a model with more specific

Table 2
Biomass (g/m^2), the proportion of energy towards respiration (*ActiveRespFrac*), and the energy lost to respiration (*ActiveRespLoss*; g/m^2) for all model versions including the static Rpath starting point for the dynamic versions. High is the high warming temperature forcing scenario, and Low is low warming scenario. In the respiration versions, the *ActiveRespFrac* is shown with the forced respiration modifier in parentheses. For the dynamic models, the value shown is the 2054 projection.

Functional group	Variable	Base	Cons High	Cons Low	Resp High	Resp Low	Rpath
Plank-tivorous Fish	Annual_Biomass	15.28	17.03	16.53	14.55	14.71	12.3
	ActiveRespFrac	0.53	0.53	0.53	0.53 (1.042)	0.53 (1.035)	0.53
	ActiveRespLoss	76.30	81.12	80.13	81.44	80.69	71.14
Benth-ivorous Fish	Annual_Biomass	10.28	12.46	11.90	9.93	10.08	9.22
	ActiveRespFrac	0.61	0.61	0.61	0.61 (1.035)	0.61 (1.030)	0.61
	ActiveRespLoss	31.51	36.14	35.27	34.39	34.10	25.31
Pisc-ivorous Fish	Annual_Biomass	6.63	8.25	7.78	9.25	8.57	2.08
	ActiveRespFrac	0.48	0.48	0.48	0.48 (0.924)	0.48 (0.932)	0.48
	ActiveRespLoss	8.42	10.20	9.81	9.45	9.18	4.61

temperature estimates or simple generalized warming trends. Because of the deterministic nature of the EwE and Rpath and the setup of the base model, we forced the models using the annually-averaged temperature trends, even though we would expect more intra-annual variability in the realized temperature. The water temperature patterns of Narragansett Bay are seasonal, reaching over 23 °C and below 0 °C, with the winter period experiencing the greatest warming trend (Fulweiler et al., 2015; Langan et al., 2021). However, the annual averaging of temperature was required to match the construction of the Innes-Gold et al. (2020) model. Future research could explore the spatial and temporal variability of temperature at finer scales, as small-scale rates of temperature change have been shown to have physiological impacts (Peck et al., 2009).

4.2. Consumption thermal response

Our results are consistent with bioenergetic theory in which warming water increases fish consumption, though the exact curve shape differs by functional group depending on the specific parameters of the Kitchell equation. Our work is also notable in that these thermal response curves were created using species-specific data in existing literature. Functional group consumption thermal response curves can be updated as more data become available. With climate change, there may be increased fish predation pressure in Narragansett Bay as average Bay temperatures are still below the temperature of optimum consumption.

The average thermal response for a functional group can shift as community composition changes, potentially mirroring the changing temperature conditions (Flanagan et al., 2019). Warming waters can restructure marine communities as species move to remain within their preferred thermal habitat (Burrows et al., 2019; Hale et al., 2017; Nicolas et al., 2011). Narragansett Bay has seen species shifts as waters have warmed over the last few decades (Collie et al., 2008; Oviatt et al., 2003). Our community composition sensitivity test showed that large interannual variability in relative species abundance can have as strong an impact on the consumption thermal response as the introduction of new species with warmer tolerances if those new species begin at relatively small biomasses.

4.3. Respiration thermal response

Our study is the first Ecosim-type model to include temperature-dependent respiration as a forcing function. The functionality of forcing *ActiveRespFrac* is now available in the Rpath R package to be used by other researchers moving forward. The methodology is flexible so that the respiration modifier can be based on the thermal response curve shape that was most appropriate for the forced group. While we did not include respiration thermal response curves based on measured field data, the Blanchard et al. (2012) parameterization of the Arrhenius equation yielded a reasonable description of changing metabolic costs for the fishes in our ecosystem. Ideally, we would have had species-specific responses, but since there were few respiration data available for the individual species in our ecosystem, we would have used assumed values regardless. Some studies report a temperature that corresponds to a maximum resting metabolism beyond which metabolic demand decreases (Bernreuther et al., 2013; MacIsaac et al., 1997; Schulte, 2015), but this decrease is not always seen (Giacomin et al., 2017; McKenzie et al., 2016; Stewart and Binkowski, 1986). Other environmental drivers, such as pH, can alter the pattern of metabolic response to temperature (Schwieterman et al., 2019). Future work could assess output sensitivity to the respiration functional form chosen, and ecosystems with more metabolic studies of their component species may be amenable to responses fitted to real data.

Our *ActiveRespFrac* values in the base version of the model (0.48–0.61) appear reasonable, though studies are limited, and the fraction of consumed energy devoted to respiration is not a frequently reported metric. Studies of other fishes have reported estimates varying from 26% to 70%, with more generalized studies estimating that respiratory costs constitute approximately half the energy budget (41–66%; Anacleto et al., 2018; Dabrowski, 1985; Priede, 1985; Sun et al., 2006). We strongly recommend ground truthing *ActiveRespFrac* values in the balancing step when building future mass-balance models to be used to examine thermal drivers and bioenergetic questions. Previous work has also found that temperature altered growth rates as a result of the balance between energy inputs and outputs (Cotton et al., 2003; Gaylord et al., 2003; Present and Conover, 1992). The production curves varied between the fish groups, and the aggregation of multiple fish species with differing data quality into a single functional group response was likely responsible for any deviations in curve shape from theory.

We provide a yearly-averaged snapshot of consumption and respiration, but increased model accuracy could be achieved with intra-annual variability in the energetic balances. The *ActiveRespFrac* for a species or functional group varies based on the environmental temperature. A warmer summer would have a larger respiratory demand than a colder winter. Therefore, the energetic balance between the seasons may determine energy storage or the annual growth (Bacon et al., 2005; Flath and Diana, 1985). Furthermore, seasonal migrations can adjust the thermal conditions experienced by an organism (Langan et al., 2021). Behavioral responses such as thermoregulation or changes in risk taking behavior add complexity to these dynamics (Nagelkerken and Munday, 2016; Neubauer and Andersen, 2019). Our setup smooths spatial and temporal variability in thermal habitat to utilize an existing model and focus on methodological development, but we believe our setup of temperature-dependent consumption and respiration is applicable to addressing questions of seasonal or spatial energetic shifts.

Mass-balance models, such as Rpath, are implicitly parameterized for ambient temperatures, and when the temperature changes, so will the vital parameters. The initial piscivorous fish life history parameters (i.e., *Q/B* and natural mortality) from Fishbase were generally estimated from warmer temperature environments which can result in higher consumption and metabolism (Froese and Pauly, 2019). Creating mass-balance models can necessitate borrowing parameter values from similar species and geographic regions, but users should consider inconsistencies in environmental conditions if they hope to include temperature impacts in their modeled ecosystem.

4.4. Comparison of model versions

Biomass projections between the model versions were noticeably different, though these differences were small due to the consistent forcing of phytoplankton and fishing mortality stabilizing the outputs. It was important to test all three model versions to isolate the effects of temperature-dependent consumption, which represented the existing capability of Rsim, and added realism of bioenergetic responses by including both temperature-dependent consumption and respiration in the respiration version of our model. The fish biomass projections were similar for 1994–2018 and diverged beyond 2018 as the temperature increased. The consumption model versions had the highest biomasses for benthivorous and planktivorous fish reflecting the increased energy intake and assuming that all of the energy was available for production. The respiration model versions had the lowest benthivorous and planktivorous fish biomasses, a result consistent with increased energetic demands of warmer waters (Chabot et al., 2016). If Narragansett Bay experiences cooler waters in the future, the opposite responses may be seen and biomasses of benthivorous and planktivorous fish may increase.

Ignoring the shifting bioenergetic balance when modeling fish biomass in response to warming waters may yield optimistic forecasts for fisheries. Models with temperature-dependent consumption only can effectively show how consumption, and therefore predation pressure on lower groups, may be altered with rising temperatures. Yet, changing temperatures can also affect the efficiency with which that increased

intake is transformed into production (Lemoine and Burkepile, 2012). Our work with both temperature-dependent consumption and respiration can be used to explore ecosystem outcomes when more energy is devoted to maintaining standard metabolic demands. Changing productivity of fish populations can potentially lead to lower sustainable fisheries yields (Free et al., 2019), and different management approaches may need to be considered when examining a warming ecosystem (Serpetti et al., 2017). As top predators, piscivorous fish likely had the smallest biomass differences between the respiration and consumption model versions because they were both externally forced with changing energetic demands, and their prey (i.e., the other fish groups) were also affected. In the respiration model versions, the respiration costs for the piscivorous fish group were decreasing, and the group might have had higher biomasses if their prey fish had not declined due to their own increasing metabolic costs. Trophic amplification of environmental impacts has been shown in other models of warming systems, where predators showed greater declines than forced declines in primary producers because the intermediate groups were also affected (Kwiatkowski et al., 2019; Lotze et al., 2019). Even limiting variable forcing to the fish groups had trickle-down effects on other groups of the ecosystem. While the changes in the biomass of other functional groups were more minor than the fish groups, they were still noticeable. Altered fisheries productivity is projected to have global ramifications on catch (Sumaila et al., 2011), and changes in growth, distribution, and trophic interactions stemming from eco-physiological consequences of warming waters are important to include when estimating fisheries production under climate change (Cheung et al., 2011). As Rsim models continue to gain popularity, we provide an additional tool to explore increased nuance in how fisheries and ecosystems may respond to climate change.

The vulnerabilities estimated for our fish groups were generally bottom-up, so the predation mortality that these fish groups can exert on their prey was limited even as fish biomass increases (Christensen and Walters, 2004). The vulnerability sensitivity test showed the influence of vulnerability parameters on Ecosim and Rsim biomass projections, which has been described by others (Heymans et al., 2016; SEDAR, 2020). Because higher (i.e., more top-down) vulnerabilities led to higher consumption and biomasses, top-down ecosystems may be more strongly affected by changing predator bioenergetics.

We chose to not refit the model versions (i.e., re-estimate vulnerabilities) after including the temperature drivers to isolate the impacts of changing bioenergetics. Therefore, while biomass projections differed, we did not necessarily achieve a better model fit with the inclusion of temperature-dependent fish bioenergetics. It is not unexpected that the respiration version of the model does not consistently have better fits even though it includes the most realism in bioenergetic response. Beside not adjusting major model fitting parameters, our model is a simplification of the system. The changing energetics may have differing interactions with the assumptions regarding seasonality, reproduction, or the directional bias of the fits of the original model. A model with vulnerabilities estimated by fitting procedures after adding the thermal responses may better match observed biomass as has been seen in other EwE models (Bentley et al., 2020, 2017), and researchers may make different decisions in original fitting if they want to optimize their model for questions of changing temperature. However, our focus was on developing new metabolic functionality in Rpath and understanding the scale at which temperature-dependent fish bioenergetics can impact predicted biomasses rather than using bioenergetic theory to explain observed trends.

4.5. Considerations for future models

This model required a vast amount of data, but data for basic bioenergetic parameters do not always exist, particularly as studies may be biased toward species of economic importance or those able to thrive in laboratory conditions (Peck et al., 2014). Physiological studies seem to emphasize the nuance of fish response to temperature. While advanced bioenergetic models may be able to capture this nuance, generalized ecosystem modeling efforts could benefit from availability of bioenergetic data captured in standard thermal response parameters or generalized species responses. Increased ability to assess parameter uncertainty could be achieved by combining this work with the Bayesian EcoSense routine (Aydin et al., 2007; Whitehouse and Aydin, 2020), or utilizing correlation analysis (Bentley et al., 2020).

We modeled simple bioenergetic responses to temperature based on established bioenergetic principles. In reality, the factors influencing consumption and metabolism are much more complex. Thermal responses can differ between individuals as well as populations, and responses can be altered by the presence of simultaneous stressors (Farrell, 2016; Kroeker et al., 2013; Present and Conover, 1992). A model with increased use of the multi-stanza feature would enhance realism with temperature-dependent consumption and growth curves for the size or age classes. A base model with enhanced size or age-structuring could address stage-specific thermal tolerances (Hare et al., 2010), the role of body size in metabolic performance (Luo and Brandt, 1993; Sibly et al., 2012), or feedbacks between temperature, reproduction, and recruitment processes (Conover and Kynard, 1981; James, 2020; Johnston et al., 1998; Pankhurst and Munday, 2011). However, a future size-structured model would require additional data to separate the original Ecopath parameters, forcing functions, and bioenergetic data for each size or age class. Finally, we did not include acclimation effects, though the previous thermal exposure of organisms can affect their response to temperature, nor the rate of temperature change, which can alter an organism's response (Morgan et al., 2018; Otto et al., 1976; Pinsky et al., 2020). We hope that future work can examine questions of thermally driven bioenergetics changes on smaller spatial or temporal scales to account for these more nuanced responses.

Our work could be expanded in the future to include thermal responses experienced by other non-fish functional groups. As phytoplankton is a single, non-size structured group, our model is not optimized to capture the complex interactions between primary production and temperature. Therefore, we chose to simplify our work by assuming static phytoplankton biomass from 2019 to 2054 which let us isolate the impact of changing top-down bioenergetics. However, climate change has been shown to influence community composition, abundance, and timing of plankton blooms (Lawrence and Menden--Deuer, 2012; Smith et al., 2010; Sullivan et al., 2001), which could have significant feedbacks on Narragansett Bay energy flow (Monaco and Ulanowicz, 1997). Reduced primary production due to climate change could result in reduced fisheries catch if lower level production can no longer support high predator abundance (Brown et al., 2010; Cheung et al., 2011; Johansen et al., 2015). Fishing and other human activities are also considered significant drivers of ecosystem indicators (Link et al., 2010). More confidence and precision in future biomass estimates could be achieved through the inclusion of the thermal responses of the lower trophic level groups and additional varying top-down and bottom-up dynamics.

6. Conclusion

Mass-balance models have most often been used to address fisheries harvest questions (Pauly et al., 2000); our work builds on previous applications of environmentally driven food web models incorporate additional climate change impacts. In our Narragansett Bay case study, we have demonstrated that the inclusion of temperature-dependent bioenergetic drivers into Rpath and Rsim models can alter projections of biomass and energy flow. Ecosystem health and sustainability goals can be better achieved by integrating principles of conservation physiology into multispecies models to gain improved resolution on how ecosystems will respond to environmental pressures (McKenzie et al., 2016). Productivity of Narragansett Bay, and similar ecosystems, may be compromised in a warmer future if fish or other ectotherms devote greater amounts of energy towards meeting metabolic demands. Our

novel methodology in Rsim is intended to serve as an example to address such questions in other warming marine ecosystems (Pershing et al., 2015) or lake environments (Adrian et al., 2009) in which there may limited ability for fish to seek alternate temperatures. The new functionality for temperature-dependent respiration in the Rpath package can be combined with other thermally-driven model components to provide the most comprehensive predictions of how a food web will respond to climate change.

CRediT authorship contribution statement

Margaret Heinichen: Conceptualization, Data curation, Investigation, Methodology, Writing – original draft. **M. Conor McManus:** Methodology, Writing – review & editing. **Sean M. Lucey:** Software, Writing – review & editing. **Kerim Aydin:** Software, Writing – review & editing. **Austin Humphries:** Funding acquisition, Resources, Writing – review & editing. **Anne Innes-Gold:** Visualization, Writing – review & editing. **Jeremy Collie:** Conceptualization, Funding acquisition, Resources, Supervision, Writing – review & editing.

Declaration of Competing Interest

The authors declare that they have no known competing financial interests or personal relationships that could have appeared to influence the work reported in this paper.

Acknowledgments

This work was supported by Rhode Island National Science Foundation Established Program to Stimulate Competitive Research Grant #OIA-165522. We acknowledge the World Climate Research Programme, which, through its Working Group on Coupled Modeling, coordinated and promoted CMIP6. We thank the climate modeling groups for producing and making available their model output, the Earth System Grid Federation (ESGF) for archiving the data and providing access, and the multiple funding agencies who support CMIP6 and ESGF. We thank those that assisted with the development of this model and for their edits on this manuscript including J. Langan, C. Suckling, and R. Bell. This work is a contribution of the Rhode Island Marine Fisheries Institute.

Supplementary materials

Supplementary material associated with this article can be found, in the online version, at doi:10.1016/j.ecolmodel.2022.109911.

References

Adrian, R., O'Reilly, C.M., Zagarese, H., Baines, S.B., Hessen, D.O., Keller, W., Livingstone, D.M., Sommaruga, R., Straile, D., Van Donk, E., Weyhenmeyer, G.A., Winder, M., 2009. Lakes as sentinels of climate change. Limnol. Oceanogr. 54, 2283–2297. https://doi.org/10.4319/lo.2009.54.6_part_2.2283.

Ahrens, R.N.M., Walters, C.J., Christensen, V., 2012. Foraging arena theory. Fish Fish. 13, 41–59. https://doi.org/10.1111/j.1467-2979.2011.00432.x.

Anacleto, P., Figueiredo, C., Baptista, M., Maulvault, A.L., Camacho, C., Pousão-Ferreira, P., Valente, L.M.P., Marques, A., Rosa, R., 2018. Fish energy budget under ocean warming and flame retardant exposure. Environ. Res. 164, 186–196. https://doi.org/10.1016/j.envres.2018.02.023.

Audzijonyte, A., Gorton, R., Kaplan, I. and Fulton, E.A. 2017. Atlantis user's guide part I: general overview, physics & ecology. CSIRO living document. Accessed December 2021. https://research.csiro.au/atlantis.

Aydin, K.Y., 2004. Age structure or functional response? Reconciling the energetics of surplus production between single-species models and ECOSIM. Afr. J. Mar. Sci. 26, 289–301. https://doi.org/10.2989/18142320409504062.

Aydin, K., Lucey, S., Gaichas, S., 2016. Rpath: R implementation of Ecopath with Ecosim.

Aydin, K.Y., Gaichas, S., Ortiz, I., Kinzey, D., Friday, N., 2007. A Comparison of the Bering Sea, Gulf of Alaska, and Aleutian Islands Large Marine Ecosystems through Food Web Modeling. U.S. Department of Commerce, NOAA Tech, Memo. NMFS-AFSC-178 298.

Bacon, P.J., Gurney, W.S.C., Jones, W., Mclaren, I.S., Youngson, A.F., 2005. Seasonal growth patterns of wild juvenile fish: partitioning variation among explanatory variables, based on individual growth trajectories of Atlantic salmon (*Salmo salar*) parr. J. Anim. Ecol. 74, 1–11.

Barange, B., Beveridge, C., Funge-Smith, P., 2018. Impacts of climate change on fisheries and aquaculture: synthesis of current knowledge, adaptation and mitigation options. Rome.

Bell, R.J., Wood, A., Hare, J., Richardson, D., Manderson, J., Miller, T., 2018. Rebuilding in the face of climate change. Can. J. Fish. Aquat. Sci. 75, 1405–1414. https://doi.org/10.1139/cjfas-2017-0085.

Bentley, J.W., Serpetti, N., Fox, C.J., Heymans, J.J., Reid, D.G., 2020. Retrospective analysis of the influence of environmental drivers on commercial stocks and fishing opportunities in the Irish Sea. Fish. Oceanogr. 29, 415–435. https://doi.org/10.1111/fog.12486.

Bentley, J.W., Serpetti, N., Heymans, J.J., 2017. Investigating the potential impacts of ocean warming on the Norwegian and Barents Seas ecosystem using a time-dynamic food-web model. Ecol. Model. 360, 94–107. https://doi.org/10.1016/j.ecolmodel.2017.07.002.

Bernreuther, M., Herrmann, J.P., Peck, M.A., Temming, A., 2013. Growth energetics of juvenile herring, *Clupea harengus L.*: food conversion efficiency and temperature dependency of metabolic rate. J. Appl. Ichthyol. 29, 331–340. https://doi.org/10.1111/jai.12045.

Blanchard, J.L., Jennings, S., Holmes, R., Harle, J., Merino, G., Allen, J.I., Holt, J., Dulvy, N.K., Barange, M., 2012. Potential consequences of climate change for primary production and fish production in large marine ecosystems. Philos. Trans. R. Soc. B Biol. Sci. 367, 2979–2989. https://doi.org/10.1098/rstb.2012.0231.

Brander, K., 2015. Improving the reliability of fishery predictions under climate change. Curr. Clim. Chang. Rep. 1, 40–48. https://doi.org/10.1007/s40641-015-0005-7.

Brett, J.R., 1971. Energetic responses of salmon to temperature. A study of some thermal relations in the physiology and freshwater ecology of sockeye salmon (*Oncorhynchus nerka*). Am. Zool. 11, 99–113. https://doi.org/10.1093/icb/11.1.99.

Brown, C.J., Fulton, E.A., Hobday, A.J., Matear, R.J., Possingham, H.P., Bulman, C., Christensen, V., Forrest, R.E., Gehrke, P.C., Gribble, N.A., Griffiths, S.P., Lozano-Montes, H., Martin, J.M., Metcalf, S., Okey, T.A., Watson, R., Richardson, A.J., 2010. Effects of climate-driven primary production change on marine food webs: implications for fisheries and conservation. Glob. Chang. Biol. 16, 1194–1212. https://doi.org/10.1111/j.1365-2486.2009.02046.x.

Brown, J.H., Gillooly, J.F., Allen, A.P., Savage, V.M., West, G.B., 2004. Toward a metabolic theory of ecology. Ecology 85, 1771–1789. https://doi.org/10.1890/03-9000.

Buchheister, A., Miller, T.J., Houde, E.D., 2017. Evaluating ecosystem-based reference points for Atlantic menhaden. Mar. Coast. Fish. 9, 457–478. https://doi.org/10.1080/19425120.2017.1360420.

Buckel, J.A., Steinberg, N.D., Conover, D.O., 1995. Effects of temperature, salinity, and fish size on growth and consumption of juvenile bluefish. J. Fish Biol. 47, 696–706. https://doi.org/10.1111/j.1095-8649.1995.tb01935.x.

Burrows, M.T., Bates, A.E., Costello, M.J., Edwards, M., Edgar, G.J., Fox, C.J., Halpern, B. S., Hiddink, J.G., Pinsky, M.L., Batt, R.D., García Molinos, J., Payne, B.L., Schoeman, D.S., Stuart-Smith, R.D., Poloczanska, E.S., 2019. Ocean community warming responses explained by thermal affinities and temperature gradients. Nat. Clim. Chang. https://doi.org/10.1038/s41558-019-0631-5.

Chabot, D., McKenzie, D.J., Craig, J.F., 2016. Metabolic rate in fishes: definitions, methods and significance for conservation physiology. J. Fish Biol. 88, 1–9. https://doi.org/10.1111/jfb.12873.

Cheung, W.W.L., Dunne, J., Sarmiento, J.L., Pauly, D., 2011. Integrating ecophysiology and plankton dynamics into projected maximum fisheries catch potential under climate change in the Northeast Atlantic. ICES J. Mar. Sci. 68, 1008–1018. https://doi.org/10.1093/icesjms/fsr012.

Christensen, V., Pauly, 1992. ECOPATH II-A software for balancing steady-state ecosystem models and calculating network characteristics. Ecol. Model. 613, 169–185. https://doi.org/10.1016/0304-3800(92)90016-8.

Christensen, V., Walters, C.J., 2004. Ecopath with Ecosim: methods, capabilities and limitations. Ecol. Model. 172, 109–139. https://doi.org/10.1016/j.ecolmodel.2003.09.003.

Christensen, V., Walters, C.J., Pauly, D., 2005. Ecopath with Ecosim: A User's Guide, Fisheries Centre. University of British Columbia, Vancouver. https://doi.org/10.1016/0304-3800(92)90016-8.

Christensen, V., Walters, C.J., Pauly, D., Forrest, R., 2008. Ecopath with Ecosim version 6 user guide.

Clarke, A., Johnston, N.M., 1999. Scaling of metabolic rate with body mass and temperature in teleost fish. J. Anim. Ecol. 68, 893–905. https://doi.org/10.1046/j.1365-2656.1999.00337.x.

Coll, M., Bundy, A., Shannon, L.J., 2009. Ecosystem modelling using the Ecopath with Ecosim approach. In: Megrey, B.A., Moksness, E. (Eds.), Computers in Fisheries Research. Springer, Dordrecht, pp. 1–421. https://doi.org/10.1007/978-1-4020-8636-6.

Colléter, M., Valls, A., Guitton, J., Gascuel, D., Pauly, D., Christensen, V., 2015. Global overview of the applications of the Ecopath with Ecosim modeling approach using the EcoBase models repository. Ecol. Model. 302, 42–53. https://doi.org/10.1016/j.ecolmodel.2015.01.025.

Collie, J.S., Wood, A.D., Jeffries, H.P., 2008. Long-term shifts in the species composition of a coastal fish community. Can. J. Fish. Aquat. Sci. 65, 1352–1365. https://doi.org/10.1139/F08-048.

Conover, D.O., Kynard, B.E., 1981. Environmental sex determination: interaction of temperature and genotype in a fish. Science 213, 577–579. https://doi.org/10.1126/science.213.4507.577.

Cooke, S.J., Killen, S.S., Metcalfe, J.D., McKenzie, D.J., Mouillot, D., Jørgensen, C., Peck, M.A., 2014. Conservation physiology across scales: insights from the marine realm. Conserv. Physiol. 2, 1–15. https://doi.org/10.1093/conphys/cou024.
Corrales, X., Coll, M., Ofir, E., Heymans, J.J., Steenbeek, J., Goren, M., Edelist, D., Gal, G., 2018. Future scenarios of marine resources and ecosystem conditions in the Eastern Mediterranean under the impacts of fishing, alien species and sea warming. Sci. Rep. 8, 14284. https://doi.org/10.1038/s41598-018-32666-x.
Corrales, X., Coll, M., Ofir, E., Piroddi, C., Goren, M., Edelist, D., Heymans, J.J., Steenbeek, J., Christensen, V., Gal, G., 2017. Hindcasting the dynamics of an Eastern Mediterranean marine ecosystem under the impacts of multiple stressors. Mar. Ecol. Prog. Ser. 580, 17–36. https://doi.org/10.3354/meps12271.
Cotton, C., Walker, R., Recicar, T., 2003. Effects of temperature and salinity on growth of Juvenile Black Sea Bass, with implications for aquaculture. N. Am. J. Aquac. 65, 330–338. https://doi.org/10.1577/c02-037.
Dabrowski, K.R., 1985. Energy budget of coregonid (*Coregonus* spp.) fish growth, metabolism and reproduction. Oikos 45. https://doi.org/10.2307/3565571.
Dahlke, F.T., Wohlrab, S., Butzin, M., Pörtner, H.O., 2020. Thermal bottlenecks in the life cycle define climate vulnerability of fish. Science 369, 65–70. https://doi.org/10.1126/science.aaz3658.
Dalla Via, J., Villani, P., Gasteiger, E., Niederstätter, H., 1998. Oxygen consumption in sea bass fingerling *Dicentrarchus labrax* exposed to acute salinity and temperature changes: metabolic basis for maximum stocking density estimations. Aquaculture 169, 303–313. https://doi.org/10.1016/S0044-8486(98)00375-5.
Dalton, T., Thompson, R., Jin, D., 2010. Mapping human dimensions in marine spatial planning and management: an example from Narragansett Bay, Rhode Island. Mar. Policy 34, 309–319. https://doi.org/10.1016/J.MARPOL.2009.08.001.
Deslauriers, D., Chipps, S.R., Breck, J.E., Rice, J.A., Madenjian, C.P., 2017. Fish bioenergetics 4.0: an R-based modeling application. Fisheries 42, 586–596. https://doi.org/10.1080/03632415.2017.1377558.
Eyring, V., Bony, S., Meehl, G.A., Senior, C.A., Stevens, B., Stouffer, R.J., Taylor, K.E., 2016. Overview of the coupled model intercomparison project phase 6 (CMIP6) experimental design and organization. Geosci. Model Dev. 9, 1937–1958. https://doi.org/10.5194/gmd-9-1937-2016.
Farrell, A.P., 2016. Pragmatic perspective on aerobic scope: peaking, plummeting, pejus and apportioning. J. Fish Biol. 88, 322–343. https://doi.org/10.1111/jfb.12789.
Flath, L.E., Diana, J.S., 1985. Seasonal energy dynamics of the Alewife in Southeastern Lake Michigan; seasonal energy dynamics of the Alewife in Southeastern Lake Michigan. Trans. Am. Fish. Soc. 114, 328–337, 10.1577/1548-8659(1985)114<328:SEDOTA>2.0.CO;2.
Flanagan, P.H., Jensen, O.P., Morley, J.W., Pinsky, M.L., 2019. Response of marine communities to local temperature changes. Ecography 42, 214–224. https://doi.org/10.1111/ecog.03961 (Cop.).
Fogarty, M.J., Collie, J.S., 2020. Fishery ecosystem dynamics, fishery ecosystem dynamics. 10.1093/oso/9780198768937.001.0001.
Free, C.M., Thorson, J.T., Pinsky, M.L., Oken, K.L., Wiedenmann, J., Jensen, O.P., 2019. Impacts of historical warming on marine fisheries production. Science 365, 979–983. https://doi.org/10.1126/science.aau1758.
Froese, F., Pauly, D., 2019. FishBase [WWW Document]. Accessed October 2020. URL http://fishbase.org/.
Fu, S.J., Zeng, L.Q., Li, X.M., Pang, X., Cao, Z.D., Peng, J.L., Wang, Y.X., 2009. The behavioural, digestive and metabolic characteristics of fishes with different foraging strategies. J. Exp. Biol. 212, 2296–2302. https://doi.org/10.1242/jeb.027102.
Fulweiler, R.W., Oczkowski, A.J., Miller, K.M., Oviatt, C.A., Pilson, M.E.Q., 2015. Whole truths vs. half-truths - and a search for clarity in long-term water temperature records. Estuar. Coast. Shelf Sci. 157, A1–A6. https://doi.org/10.1016/j.ecss.2015.01.021.
Gaylord, T.G., Schwarz, M.H., Cool, R.W., Jahncke, M.L., Craig, S.R., 2003. Thermal optima for the culture of juvenile summer flounder, *Paralichthys dentatus*. J. Appl. Aquac. 14, 155–162. https://doi.org/10.1300/J028v14n03_12.
Giacomin, M., Schulte, P.M., Wood, C.M., 2017. Differential effects of temperature on oxygen consumption and branchial fluxes of urea, ammonia, and water in the dogfish shark (*Squalus acanthias suckleyi*). Physiol. Biochem. Zool. 90, 627–637. https://doi.org/10.1086/694296.
Gillooly, J.F., Brown, J.H., West, G.B., Savage, V.M., Charnov, E.L., 2001. Effects of size and temperature on metabolic rate. Science 293, 2248–2251. https://doi.org/10.1126/science.1061967.
Guénette, S., Araújo, J.N., Bundy, A., 2014. Exploring the potential effects of climate change on the Western Scotian Shelf ecosystem, Canada. J. Mar. Syst. 134, 89–100. https://doi.org/10.1016/J.JMARSYS.2014.03.001.
Guénette, S., Heymans, S.J.J., Christensen, V., Trites, A.W, 2006. Ecosystem models show combined effects of fishing, predation, competition, and ocean productivity on Steller sea lions (*Eumetopias jubatus*) in Alaska. Can. J. Fish. Aquat. Sci. 63, 2495–2517. https://doi.org/10.1139/F06-136.
Hale, S.S., Buffum, H.W., Kiddon, J.A., Hughes, M.M., 2017. Subtidal benthic invertebrates shifting northward along the US Atlantic Coast. Estuaries Coasts 40, 1744–1756. https://doi.org/10.1007/s12237-017-0236-z.
Hansen, P., Johnson, T., Schindler, D.E., Kitchell, J., 1997. Fish Bioenergetics 3.0 Manual. Fish Bioenerg. 3.0.
Hansson, S., Rudstam, L.G., Kitchell, J.F., Hildén, M., Johnson, B.L., Peppard, P.E., 1996. Predation rates by North Sea cod (*Gadus morhua*) - predictions from models on gastric evacuation and bioenergetics. ICES J. Mar. Sci. 53 https://doi.org/10.1006/jmsc.1996.0010.
Hare, J.A., Alexander, M.A., Fogarty, M.J., Williams, E.H., Scott, J.D., 2010. Forecasting the dynamics of a coastal fishery species using a coupled climate-population model. Ecol. Appl. 20, 452–464. https://doi.org/10.1890/08-1863.1.
Hartman, K.J., Brandt, S.B., 1995. Comparative energetics and the development of bioenergetics models for sympatric estuarine piscivores. Can. J. Fish. Aquat. Sci. 52, 1647–1666. https://doi.org/10.1139/f95-759.
Harvey, C.J., 2009. Effects of temperature change on demersal fishes in the California current: a bioenergetics approach. Can. J. Fish. Aquat. Sci. 66, 1449–1461. https://doi.org/10.1139/F09-087.
Hernvann, P.Y., Gascuel, D., Grüss, A., Druon, J.N., Kopp, D., Perez, I., Piroddi, C., Robert, M., 2020. The Celtic sea through time and space: ecosystem modeling to unravel fishing and climate change impacts on food-web structure and dynamics. Front. Mar. Sci. 7 https://doi.org/10.3389/fmars.2020.578717.
Heymans, J.J., Coll, M., Link, J.S., Mackinson, S., Steenbeek, J., Walters, C., Christensen, V., 2016. Best practice in Ecopath with Ecosim food-web models for ecosystem-based management. Ecol. Model. 331, 173–184. https://doi.org/10.1016/j.ecolmodel.2015.12.007.
Heymans, S.J., Guénette, S., Christensen, V., Trites, A.W., 2005. Changes in Gulf of Alaska ecosystems due to ocean climate change and fishing. ICES CM M22. https://doi.org/10.1016/j.ecolmodel.2008.06.013.
Humphries, Murray, McCann, Kevin, 2014. Metabolic Ecology. Journal of Animal Ecology 83 (1), 7–19. https://doi.org/10.1111/1365-2656.12124.
Innes-Gold, A., Heinichen, M., Gorospe, K., Truesdale, C., Collie, J., Humphries, A., 2020. Modeling 25 years of food web changes in Narragansett Bay (USA) as a tool for ecosystem-based management. Mar. Ecol. Prog. Ser. 654, 17–33. https://doi.org/10.3354/meps13505.
Innes-Gold, A., Pavlowich, T., Heinichen, M., McManus, M.C., McNamee, J., Collie, J., Humphries, A., 2021. Exploring social-ecological trade-offs in fisheries using a coupled food web and human behavior model. Ecol. Soc. https://doi.org/10.5751/ES-12451-260240, 26 Publ. online Jun 18, 2021.
James, K.C., 2020. Vertebral growth and band-pair deposition in sexually mature little skates *Leucoraja erinacea*: is adult band-pair deposition annual? J. Fish Biol. 96, 4–13. https://doi.org/10.1111/jfb.14141.
Jobling, M., 1997. Temperature and growth: modulation of growth rate via temperature change. In: Wood, C.M., McDonald, D.G. (Eds.), Global Warming Implications for Freshwater and Marine Fish. Cambridge University Press, pp. 225–254. https://doi.org/10.1017/CBO9780511983375.
Jobling, M., 1994. Fish Bioenergetics, 1st ed. Chapman & Hall.
Johansen, J.L., Jones, G.P., 2011. Increasing ocean temperature reduces the metabolic performance and swimming ability of coral reef damselfishes. Glob. Chang. Biol. 17, 2971–2979. https://doi.org/10.1111/j.1365-2486.2011.02436.x.
Johansen, J.L., Messmer, V., Coker, D.J., Hoey, A.S., Pratchett, M.S., 2014. Increasing ocean temperatures reduce activity patterns of a large commercially important coral reef fish. Glob. Chang. Biol. 20, 1067–1074. https://doi.org/10.1111/gcb.12452.
Johansen, J.L., Pratchett, M.S., Messmer, V., Coker, D.J., Tobin, A.J., Hoey, A.S., 2015. Large predatory coral trout species unlikely to meet increasing energetic demands in a warming ocean. Sci. Rep. 5, 1–8. https://doi.org/10.1038/srep13830.
Johnston, I.A., Cole, N.J., Abercromby, M., Vierira, V.L.A., 1998. Embryonic temperature modulates muscle growth characteristics in larval and juvenile herring. J. Exp. Biol. 201, 623–646.
Kaschner, K., Kesner-Reyes, K., Garilao, C., Rius-Barile, J., Rees, T., Froese, R., 2019. Aquamaps: predicted range maps for aquatic species. [WWW Document]. Accessed October 2020. URL https://www.aquamaps.org/.
Jørgensen, C, Enberg, K, Mangel, M, 2016. Modelling and interpreting fish bioenergetics: a role for behaviour, life-history traits and survival trade-offs. Journal of Fish Biology 88 (1), 389–402. https://doi.org/10.1111/jfb.12834.
Kearney, K.A., 2017. Ecopath_Matlab: a Matlab-based implementation of the Ecopath food web algorithm. J. Open Source Softw. 2, 64. https://doi.org/10.21105/joss.00064.
Kitchell, J.F., Stewart, D.J., Weininger, D., 1977. Applications of a bioenergetics model to yellow perch (*Perca flavescens*) and walleye (*Stizostedion vitreum vitreum*). J. Fish. Res. Board Canada 34. https://doi.org/10.1139/f77-258.
Kleisner, K.M., Fogarty, M.J., McGee, S., Hare, J.A., Moret, S., Perretti, C.T., Saba, V.S., 2017. Marine species distribution shifts on the U.S. Northeast Continental Shelf under continued ocean warming. Prog. Oceanogr. 153, 24–36. https://doi.org/10.1016/j.pocean.2017.04.001.
Kroeker, K.J., Kordas, R.L., Crim, R., Hendriks, I.E., Ramajo, L., Singh, G.S., Duarte, C.M., Gattuso, J., 2013. Impacts of ocean acidification on marine organisms: quantifying sensitivities and interaction with warming. Glob. Chang. Biol. 19, 1884–1896. https://doi.org/10.1111/gcb.12179.
Kwiatkowski, L., Aumont, O., Bopp, L., 2019. Consistent trophic amplification of marine biomass declines under climate change. Glob. Chang. Biol. 25, 218–229. https://doi.org/10.1111/gcb.14468.
Langan, J., Puggioni, G., Oviatt, C., Henderson, M., Collie, J., 2021. Climate alters the migration phenology of coastal marine species. Mar. Ecol. Prog. Ser. 660, 1–18. https://doi.org/10.3354/meps13612.
Lawrence, C., Menden-Deuer, S., 2012. Drivers of protistan grazing pressure: seasonal signals of plankton community composition and environmental conditions. Mar. Ecol. Prog. Ser. 459, 39–52. https://doi.org/10.3354/meps09771.
Lemoine, N.P., Burkepile, D.E., 2012. Temperature-induced mismatches between consumption and metabolism reduce consumer fitness. Ecology 93, 2483–2489. https://doi.org/10.1890/12-0375.1.
Link, J.S., Yemane, D., Shannon, L.J., Coll, M., Shin, Y.J., Hill, L., Borges, M.F., 2010. Relating marine ecosystem indicators to fishing and environmental drivers: an elucidation of contrasting responses. ICES J. Mar. Sci. 67, 787–795. https://doi.org/10.1093/icesjms/fsp258.
Lotze, H.K., Tittensor, D.P., Bryndum-Buchholz, A., Eddy, T.D., Cheung, W.W.L., Galbraith, E.D., Barange, M., Barrier, N., Bianchi, D., Blanchard, J.L., Bopp, L., Büchner, M., Bulman, C.M., Carozza, D.A., Christensen, V., Coll, M., Dunne, J.P.,

Fulton, E.A., Jennings, S., Jones, M.C., Mackinson, S., Maury, O., Niiranen, S., Oliveros-Ramos, R., Roy, T., Fernandes, J.A., Schewe, J., Shin, Y.J., Silva, T.A.M., Steenbeek, J., Stock, C.A., Verley, P., Volkholz, J., Walker, N.D., Worm, B., 2019. Global ensemble projections reveal trophic amplification of ocean biomass declines with climate change. Proc. Natl. Acad. Sci. U. S. A. 116, 12907–12912. https://doi.org/10.1073/pnas.1900194116.

Lucey, S.M., 2019. Improving the Ecosystem Modeling Toolbox with an Open Source Mass Balance Model. University of Massachusetts Dartmouth.

Lucey, S.M., Gaichas, S.K., Aydin, K.Y., 2020. Conducting reproducible ecosystem modeling using the open source mass balance model Rpath. Ecol. Model. 427, 109057 https://doi.org/10.1016/j.ecolmodel.2020.109057.

Luo, J., Brandt, S.B., 1993. Bay anchovy Anchoa mitchilli production and consumption in mid- Chesapeake Bay based on a bioenergetics model and acoustic measures of fish abundance. Mar. Ecol. Prog. Ser. 98, 223–236. https://doi.org/10.3354/meps098223.

MacIsaac, P.F., Goff, G.P., Speare, D.J., 1997. Comparison of routine oxygen consumption rates of three species of pleuronectids at three temperatures. J. Appl. Ichthyol. 13, 171–176. https://doi.org/10.1111/j.1439-0426.1997.tb00117.x.

McKenzie, D.J., Axelsson, M., Chabot, D., Claireaux, G., Cooke, S.J., Corner, R.A., De Boeck, G., Domenici, P., Guerreiro, P.M., Hamer, B., Jørgensen, C., Killen, S.S., Lefevre, S., Marras, S., Michaelidis, B., Nilsson, G.E., Peck, M.A., Perez-Ruzafa, A., Rijnsdorp, A.D., Shiels, H.A., Steffensen, J.F., Svendsen, J.C., Svendsen, M.B.S., Teal, L.R., van der Meer, J., Wang, T., Wilson, J.M., Wilson, R.W., Metcalfe, J.D., 2016. Conservation physiology of marine fishes: state of the art and prospects for policy. Conserv. Physiol. 4 https://doi.org/10.1093/conphys/cow046 cow046.

McManus, M.C., Ullman, D.S., Rutherford, S.D., Kincaid, C., 2020. Northern quahog (*Mercenaria mercenaria*) larval transport and settlement modeled for a temperate estuary. Limnol. Oceanogr. 289–303. https://doi.org/10.1002/lno.11297.

Monaco, M.E., Ulanowicz, R.E., 1997. Comparative ecosystem trophic structure of three U.S. mid-Atlantic estuaries. Mar. Ecol. Prog. Ser. 161, 239–254. https://doi.org/10.3354/meps161239.

Morgan, R., Finnøen, M.H., Jutfelt, F., 2018. CTmax is repeatable and doesn't reduce growth in zebrafish. Sci. Rep. 8, 1–8. https://doi.org/10.1038/s41598-018-25593-4.

Muhling, B.A., Gaitán, C.F., Stock, C.A., Saba, V.S., Tommasi, D., Dixon, K.W., 2018. Potential salinity and temperature futures for the Chesapeake Bay using a statistical downscaling spatial disaggregation framework. Estuaries Coasts 41, 349–372. https://doi.org/10.1007/s12237-017-0280-8.

Nagelkerken, I., Munday, P.L., 2016. Animal behaviour shapes the ecological effects of ocean acidification and warming: moving from individual to community-level responses. Glob. Chang. Biol. 22, 974–989. https://doi.org/10.1111/gcb.13167.

Neubauer, P., Andersen, K.H., 2019. Thermal performance of fish is explained by an interplay between physiology, behaviour and ecology. Conserv. Physiol. 7, 1–14. https://doi.org/10.1093/conphys/coz025.

Nicolas, D., Chaalali, A., Drouineau, H., Lobry, J., Uriarte, A., Borja, A., Boët, P., 2011. Impact of global warming on European tidal estuaries: some evidence of northward migration of estuarine fish species. Reg. Environ. Chang. 11, 639–649. https://doi.org/10.1007/s10113-010-0196-3.

Nowicki, J.P., Miller, G.M., Munday, P.L., 2012. Interactive effects of elevated temperature and CO2 on foraging behavior of juvenile coral reef fish. J. Exp. Mar. Biol. Ecol. 412, 46–51. https://doi.org/10.1016/j.jembe.2011.10.020.

O'Neill, B.C., Tebaldi, C., Van Vuuren, D.P., Eyring, V., Friedlingstein, P., Hurtt, G., Knutti, R., Kriegler, E., Lamarque, J.F., Lowe, J., Meehl, G.A., Moss, R., Riahi, K., Sanderson, B.M., 2016. The scenario model intercomparison project (ScenarioMIP) for CMIP6. Geosci. Model Dev. 9, 3461–3482. https://doi.org/10.5194/gmd-9-3461-2016.

Olla, B., Studholme, A., Bejda, A., 1985. Behavior of juvenile bluefish *Pomatomus saltatrix* in vertical thermal gradients: influence of season, temperature acclimation and food. Mar. Ecol. Prog. Ser. 23, 165–177. https://doi.org/10.3354/meps023165.

Otto, R.G., Kitchel, M.A., Rice, J.O., 1976. Lethal and preferred temperatures of the Alewife (*Alosa pseudoharengus*) in Lake Michigan. Trans. Am. Fish. Soc. 105, 96–106. https://doi.org/10.1577/1548-8659(1976)105≤96:laptot≥2.0.co;2.

Oviatt, Candace, Olsen, Steven, Andrews, Mark, Collie, Jeremy, Lynch, Timothy, Raposa, Kenneth, 2003. A Century of Fishing and Fish Fluctuations in Narragansett Bay. Reviews in Fisheries Science 11 (3), 221–242. https://doi.org/10.1080/10641260390244413.

Oviatt, C., Smith, L., Krumholz, J., Coupland, C., Stoffel, H., Keller, A., McManus, M.C., Reed, L., 2017. Managed nutrient reduction impacts on nutrient concentrations, water clarity, primary production, and hypoxia in a north temperate estuary. Estuar. Coast. Shelf Sci. 199, 25–34. https://doi.org/10.1016/j.ecss.2017.09.026.

Pankhurst, N.W., Munday, P.L., 2011. Effects of climate change on fish reproduction and early life history stages. Mar. Freshw. Res. 62, 1015–1026. https://doi.org/10.1071/MF10269.

Pauly, D., Christensen, V., Walters, C., Pauly, D., Walters, C., 2000. Ecopath, Ecosim, and Ecospace as tools for evaluating ecosystem impact of fisheries. ICES J. Mar. Sci. 57, 697–706. https://doi.org/10.1006/jmsc.2000.0726.

Peck, L.S., 2011. Organisms and responses to environmental change. Mar. Genom. 4, 237–243. https://doi.org/10.1016/j.margen.2011.07.001.

Peck, L.S., Clark, M.S., Morley, S.A., Massey, A., Rossetti, H., 2009. Animal temperature limits and ecological relevance: effects of size, activity and rates of change. Funct. Ecol. 23, 248–256. https://doi.org/10.1111/j.1365-2435.2008.01537.x.

Peck, L.S., Morley, S.A., Richard, J., Clark, M.S., 2014. Acclimation and thermal tolerance in Antarctic marine ectotherms. J. Exp. Biol. 217, 16–22. https://doi.org/10.1242/jeb.089946.

Pershing, A.J., Alexander, M.A., Hernandez, C.M., Kerr, L.A., Le Bris, A., 2015. Slow adaptation in the face of rapid warming leads to collapse of the Gulf of Maine cod fishery. Science 350, 809–812. https://doi.org/10.1126/science.aac9819.

Pinsky, M.L., Selden, R.L., Kitchel, Z.J., 2020. Climate-driven shifts in marine species ranges: scaling from organisms to communities. Ann. Rev. Mar. Sci. 12, 153–179. https://doi.org/10.1146/annurev-marine-010419.

Polovina, J.J., 1984. Model of a coral reef ecosystem - I. The ecopath model and its application to French Frigate Shoals. Coral Reefs 3, 1–11. https://doi.org/10.1007/BF00306135.

Present, T.M.C., Conover, D.O., 1992. Physiological basis of latitudinal growth differences in *Menidia menidia*: variation in consumption or efficiency? Funct. Ecol. 6, 23–31.

Priede, I.G., 1985. Metabolic scope in fishes. Fish Energetics. Springer, Dordrecht, pp. 33–64. https://doi.org/10.1007/978-94-011-7918-8_2.

R Core Team, 2019. R: a language and environment for statistical computing.

Ries, R., Perry, S., 1995. Potential effects of global climate warming on brook trout growth and prey consumption in central Appalachian streams, USA. Clim. Res. 5, 197–206. https://doi.org/10.3354/cr005197.

Roessig, J.M., Woodley, C.M., Cech, J.J., Hansen, L.J., 2004. Effects of global climate change on marine and estuarine fishes and fisheries. Rev. Fish Biol. Fish. 14, 251–275.

Sandersfeld, T., Mark, F.C., Knust, R., 2017. Temperature-dependent metabolism in Antarctic fish: do habitat temperature conditions affect thermal tolerance ranges? Polar Biol. 40, 141–149. https://doi.org/10.1007/s00300-016-1934-x.

Schulte, P.M., 2015. The effects of temperature on aerobic metabolism: towards a mechanistic understanding of the responses of ectotherms to a changing environment. J. Exp. Biol. 218, 1856–1866. https://doi.org/10.1242/jeb.118851.

Schwieterman, G.D., Crear, D.P., Anderson, B.N., Lavoie, D.R., Sulikowski, J.A., Bushnell, P.G., Brill, R.W., 2019. Combined effects of acute temperature change and elevated pCO_2 on the metabolic rates and hypoxia tolerances of clearnose skate (*Rostaraja eglanteria*), summer flounder (*Paralichthys dentatus*), and thorny skate (*Amblyraja radiata*). Biology 8. https://doi.org/10.3390/biology8030056 (Basel).

SEDAR, 2020. Atlantic menhaden ecological reference points stock assessment report, SEDAR 69. North Charleston, SC.

Serpetti, N., Baudron, A.R., Burrows, M.T., Payne, B.L., Helaouët, P., Fernandes, P.G., Heymans, J.J., 2017. Impact of ocean warming on sustainable fisheries management informs the ecosystem approach to fisheries. Sci. Rep. 7, 1–15. https://doi.org/10.1038/s41598-017-13220-7.

Sibly, R.M., Brown, J.H., Kodric-Brown, A., 2012. Metabolic Ecology: A Scaling Approach, 1st ed. John Wiley & Sons, Ltd. https://doi.org/10.1002/9781119968535.

Slesinger, E., Andres, A., Young, R., Seibel, B., Saba, V., Phelan, B., Rosendale, J., Wieczorek, D., Saba, G., 2019. The effect of ocean warming on black sea bass (*Centropristis striata*) aerobic scope and hypoxia tolerance. PLoS One 14, e0218390. https://doi.org/10.1371/journal.pone.0218390.

Smith, L.M., Whitehouse, S., Oviatt, C.A., 2010. Impacts of climate change on Narragansett Bay. Northeast. Nat. 17, 77–90. https://doi.org/10.1656/045.017.0106.

Stewart, D.J., Binkowski, F.P., 1986. Dynamics of consumption and food conversion by Lake Michigan Alewives: an energetics-modeling synthesis. Trans. Am. Fish. Soc. 115, 643–661.

Sullivan, B.K., Van Keuren, D., Clancy, M., 2001. Timing and size of blooms of the ctenophore Mnemiopsis Leidyi in relation to temperature in Narragansett Bay, RI, hydrobiologia.

Sumaila, U.R., Cheung, W.W.L., Lam, V.W.Y., Pauly, D., Herrick, S., 2011. Climate change impacts on the biophysics and economics of world fisheries. Nat. Clim. Chang. https://doi.org/10.1038/nclimate1301.

Sun, L., Chen, H., Huang, L., 2006. Effect of temperature on growth and energy budget of juvenile cobia (*Rachycentron canadum*). Aquaculture 261, 872–878. https://doi.org/10.1016/j.aquaculture.2006.07.028.

University of Rhode Island Graduate School of Oceanography, 2021. Fish trawl methods. [WWW Document]. Accessed March 2021. URL https://web.uri.edu/gso/research/fish-trawl/methods/.

Villasante, S., Arreguín-Sánchez, F., Heymans, J.J., Libralato, S., Piroddi, C., Christensen, V., Coll, M., 2016. Modelling marine ecosystems using the Ecopath with Ecosim food web approach: new insights to address complex dynamics after 30 years of developments. Ecol. Model. 331, 1–4. https://doi.org/10.1016/j.ecolmodel.2016.04.017.

Volkoff, H., Rønnestad, I., 2020. Effects of temperature on feeding and digestive processes in fish. Temperature 7, 307–320. https://doi.org/10.1080/23328940.2020.1765950.

Walters, C.J., Christensen, V., Pauly, D., 1997. Structuring dynamic models of exploited ecosystems from trophic mass-balance assessments. Rev. Fish Biol. Fish. 7, 139–172.

Walters, C., Christensen, V., 2007. Adding realism to foraging arena predictions of trophic flow rates in Ecosim ecosystem models: shared foraging arenas and bout feeding. Ecol. Model. 209, 342–350. https://doi.org/10.1016/j.ecolmodel.2007.06.025.

Whitehouse, G.A., Aydin, K.Y., 2020. Assessing the sensitivity of three Alaska marine food webs to perturbations: an example of Ecosim simulations using Rpath. Ecol. Model. 429, 109074 https://doi.org/10.1016/j.ecolmodel.2020.109074.